2022-12-01

Two Novel Piperidone Compounds Display Antiproliferative Effects On Human Prostate And Lymphoma Cancer Cell Lines And In Vitro Investigation Of Thiophenecarboxylate Anti-Cancer Activity

Risa Mia Swain
University of Texas at El Paso

TWO NOVEL PIPERIDONE COMPOUNDS DISPLAY ANTIPROLIFERATIVE EFFECTS ON HUMAN PROSTATE AND LYMPHOMA CANCER CELL LINES AND *IN VITRO* INVESTIGATION OF THIOPHENECARBOXYLATE ANTI-CANCER ACTIVITY

Risa Mia Swain

Doctoral Program in Biosciences

APPROVED:

_____
Renato J. Aguilera, Ph.D., Chair

_____
Guilio Francia, Ph.D.

_____
Manuel Miranda-Arango, Ph.D.

_____
Md Nurunnabi, Ph.D.

_____
Charles Spencer, Ph.D.

_____
Stephen L. Crites, Jr., Ph.D.
Dean of the Graduate School

TWO NOVEL PIPERIDONE COMPOUNDS DISPLAY ANTIPROLIFERATIVE EFFECTS ON HUMAN PROSTATE AND LYMPHOMA CANCER CELL LINES AND *IN VITRO* INVESTIGATION OF THIOPHENECARBOXYLATE ANTI-CANCER ACTIVITY

by

Risa Mia Swain, B.S.

DISSERTATION

Presented to the Faculty of the Graduate School of

The University of Texas at El Paso

in Partial Fulfillment

of the Requirements

for the Degree of

DOCTOR OF PHILOSOPHY

Department of Biological Sciences

THE UNIVERSITY OF TEXAS AT EL PASO

December 2022

ACKNOWLEDGMENTS

First and foremost, I would like to thank Dr. Aguilera for giving me the opportunity to work in his lab. It has been a difficult and humbling process. I have learned so much and grown as a scientist. I appreciate the difficult conversations that we had because it made me strive to be better.

Dr. Varela, I cannot express how grateful I am that the lab has you. You are such a kind person and you are always so open to helping. You helped me understand so many things when I was confused or needed guidance. You provided a lot of insight on subjects I was not an expert in. I value the knowledge that you shared with me. You have taught me so much and I will forever be thankful for you. Thank you from the bottom of my heart for helping me with my paper when I had no idea where to begin. You were there to tell how to make the figures look better or what would sound better. Without your help I wouldn't be where I am today. You are so great. Thank you thank you.

Denisse, where do I honestly begin. If it wasn't for you, I wouldn't have been successful in any of my experiments. Heck, I wouldn't have been successful at all in graduate school. Thank you for guiding me and showing me how to do things the proper way. Thank you for taking the time to explain things to me, even if that was the 3rd time explaining it. You were always so very patient and kind and I appreciated that so much. I appreciate the times where you would sit down and answer questions I had about a project or data. Thank you for everything.

To my friends, you know who you are. Thank you for lending an ear when I needed it the most. Thank you for listening to me through my meltdowns and frustration. Thank you for being my outlet. Most importantly, thank you for always listening to any question I had on an experiment or on a paper. Thank you for being in my life. I love you all.

To my father, I don't think you'd ever be able to understand the magnitude of love and appreciation I have for you. You have helped me so much through my academic career I cannot put it in words other than thank you. Thank you for being so stern and motivating when I needed it the most. Thank you for lighting a fire in me when it had burnt out. Thank you for always listening and never judging. Thank you for the advice. Thank you for everything. All I wanted to do was make you proud and I hope I did that.

To my mother, I appreciate you and everything you've done in my adulthood. You've gotten me through a lot. You've been there at times without question. I will forever appreciate that.

To my brother, thank you for putting up with me. I know you know what I mean but also, thank you for setting the bar high. Thank you for becoming someone I can look up too and be proud to say who you are and how far you've come. Thank you for motivating me to be better. You mean so very much to me. I hope you know that. Just so you know, being a doctor is way cooler than being a pilot. Just saying.

To my partner, thank you for roughing it out with me all these years. It's been a journey but I wouldn't trade it for anything in the world. I hope you know that I love and appreciate everything you do for me and the boys. Thank you for being my rock and

motivating me. Thank you for pushing me when I wanted to give up. Thank you for supporting me and all of my ridiculous ideas. You're my other half. Awoo wooo.

To my little monsters, Aiden and Oliver, just know that I did this for you. It was hard and I wanted to give up so many times. It's difficult going to graduate school and having children but I did it. I did it. I hope when you're older you can read this and I appreciate what I did for you guys. You guys were my motivation.

My deepest love and gratitude to you all. I would not have been able to do it if it wasn't for you all. I am forever in your dept.

ABSTRACT

Tumor interactions predominantly dominate cancer progression and its tumor microenvironment. Such interactions include, tumors generating signals that cause dysfunction and death to immune cells [1]. Inflammatory and immune cells present to eliminate cancer cells fail and lose their overall function [1]. These cells lose the overall ability to aid and are co-opted to promote tumor growth. Ultimately, the result is escaping from the hosts' immune system and developing a complex mechanism that evades immune cells and the inability to undergo apoptosis. It is imperative to develop a better understanding of the complex machinery cancer develops. There are current therapies that are being utilized to treat cancer. Some of which include surgery, radiation, chemotherapy, immunotherapy, hormone therapy, etc. [2]. Said treatments had been proven to work in some cases. However, individuals that have received chemotherapy or radiation to the chest can develop heart problems post-treatment [3]. The overall impact of chemotherapy, radiation, and any other treatment can be more detrimental than that disease itself with long-lasting effects. There are treatments that target not only the cancer cells but normal cells as well, making it a difficult process. Other treatments are only specific for certain genes, targeting a small percentage of individuals. The need for alternative novel treatments is present. It has been shown that there are novel compounds undergoing testing through high-throughput drug screening that possess favorable cytotoxic and selective effects.

Cancer is continuously affecting the lives of millions of people annually. It is the second leading cause of death and the disparities alone raise importance of investigating alternative methods to treat the disease. The process of drug discovery

has transformed in the past decade. It is now of great importance to investigate the mechanism of action at which said compounds induce cancer cell death. By doing this, it will provide great insight on how drug discovery can affect different pathways in the cell and how we can take an alternative approach to overcoming cancer. Previously published works have reported cytotoxic effects of piperidone compounds. It has been shown some piperidone compounds induce cell death by the intrinsic apoptotic pathway and inhibit the proteasome. Cancer cells utilize the proteasome to degrade proteins and various transcription factors to aid in their over proliferation. In this project, the mechanism of two piperidone compounds and one thiophenecarboxylate will be described. Detailed in this dissertation is the mechanism of death, proteasome inhibition of the piperidone compounds, and investigation of the thiophenecarboxylate that could potentially be used in future anticancer therapy.

TABLE OF CONTENTS

LIST OF TABLES

LIST OF FIGURES

ABBREVIATIONS

CC_{50}	Cytotoxic concentration 50%
DMSO	Dimethyl sulfoxide
DNS	Differential nuclear staining
DUB	Deubiquitinases
FITC	Fluorescein isothiocyanate
H_20_2	Hydrogen peroxide
NIM-DAPI	Nuclear isolation medium (NIM)-4, 6-diamidino-2-phenylindole (DAPI)
PEG	Polyethylene glycol
PI	Propidium Iodide
ROS	Reactive oxygen species
SCI	Selective cytotoxicity index
$UCHL_5$	Ubiquitin C-terminal Hydrolase L_5
UPS	Ubiquitin-Proteasome System
USP	Ubiquitin-Specific Protease

CHAPTER 1: INTRODUCTION TO CANCER

1.1 General Introduction

1.2 Cancer Statistics

It was estimated that in 2022, there would be approximately 1.9 million new cancer cases diagnosed and 609,360 cancer deaths in the United States alone [4]. It is the second leading cause of death amongst the population in the United States overall [4]. Naturally, cancer does not discriminate and affects every ethnicity, gender, and age. Many other external factors can come into play, such as genetics, diet, frequency of physical activity, weight, and smoking. For the Hispanic population, it is the leading cause of death, affecting 11% of Hispanics in the United States [5,6]. With lung, prostate, colorectal cancer being the leading cause of mortality amongst Hispanic males [5]. Among women, breast or lung cancer is either the first or second leading cause of death [5]. With colorectal cancer being the second leading cause of cancer-related death in the United States and is most commonly diagnosed in men [7]. In 2022, it was projected that 151,030 new cases of colorectal cancer would arise, causing 52,580 deaths by the end of 2022 [4].

Leukemia is the most common type of cancer in children younger than 20 years [8]. In 2022, it is projected that 60,659 male and female will be diagnosed with Leukemia and 24,000 will succumb to the illness [4]. The highest rates of childhood leukemia have been known to be children of Hispanic ethnicity [8]. Statistically, Hispanic children experience a higher age-adjusted incidence rate for acute lymphoblastic leukemia than all other demographic groups [8]. Approximately 30% of both male and female Hispanics will be diagnosed with cancer at some point in their lifetime [9].

1.3 Cancer contributing factors

Cancer disparities interplay among an array of factors including health, biology, behavior, and genetics [10]. All of which have negative effects on health, thus leading to cancer outcomes. Certain groups in the United States have an increase in cancer disparities due to low income, low health literacy, poor diets, obesity, and being physically inactive [10]. In terms of genetics, evidence suggests that there are differences in racial/ethnic groups like African Americans in regard to triple-negative breast, colorectal, and prostate cancer [10]. Differences amongst populations contribute to the lack of diversity in clinical research and therefore, need to be studied in depth [10].

1.4 Cancer characteristics

Cancer results from the proliferation of different cells in the body. A tumor is an abnormal mass of cells that can either be malignant or benign [11]. A benign

tumor most commonly resides confined to its original location, never invading the surrounding normal tissue [11]. A malignant tumor is capable of invading surrounding normal tissue and spreading throughout the whole body [11]. Both tumor types are classified from the type of cell they originate from. To promote malignant transformation a series of events need to occur. Tumor initiation is the genetic alteration of a single cell. This alteration can cause DNA damage and alter a nucleotide sequence that can lead to the expression of dysfunctional proteins [12]Damage to the DNA is critical for cancer cell progression and genome instability is what causes the progression of the disease. When the damage to the DNA has occurred, the possibility of mutations

generated increases [13]. In normal cells, endoplasmic reticulum (ER) stress from misfolded or unfolded proteins ultimately lead to apoptosis [14]. However, cancer cells possess the capability of bypassing regulatory mechanisms, such as the unfolded protein response (UPR), that degrade misfolded proteins. Certain components in the cell indirectly aid the pathogenesis of cancer, the ubiquitin-proteasome system (UPS) [15]. These are some inherent qualities that allow cancer cells to survive.

1.5 Targeting cancer

Targeted therapy is a type of treatment that is designed to target cancer without affecting surrounding normal tissue [16] Researchers have learned the environment in which cancer cells grow differ from certain cancer types [16] Some cancer cells inhibit the proteasome that ultimately leads to the accumulation of misfolded or unfolded proteins causing proteotoxic stress [17] This proteotoxic stress occurs when misfolded protein accumulation overwhelms cellular protein quality control mechanisms involving the proteasome and autophagy [17] With that being said, certain therapeutic approaches can be used to target the proteasome. Cancer cells manipulate cellular programs normally used in growth and development displaying a stress phenotype [17] Stress phenotypes are common for tumorigenesis and includes high levels of reactive oxygen species, oxidative, proteotoxic, and DNA damage stress [17]Therapies including redox state imbalances have proven to be effective [17] These variety of mechanisms can be utilized to target cancer cells.

1.6 Significance

The current anticancer therapies available include chemotherapy, immunotherapy, radiation, hormone therapy, and surgery [2]. Such therapies can be seen as redundant and overused. Most treatments, such as radiation or chemotherapy, can leave an individual with long-lasting adverse side effects post-cancer treatment. With this in mind, it is beneficial to explore alternative methods regarding treatment. Cancer cell lines have played a prominent role in the initial stages of drug discovery, facilitating the screening of thousands of compounds of potential drug targets [12]. These alternative methods, drug screening, include the screening of potential novel therapeutic agents. It has been shown that piperidone compounds possess inhibitory effects on the growth of cultured cancer cells, and many have a beneficial impact on human cancer cells [13]. In our previously published works, it has been shown piperidone compounds possess the ability to induce apoptosis through the intrinsic apoptotic pathway and display proteasome inhibition [20].Here we will demonstrate two piperidone compounds that show effective cytotoxicity on various human cancer cell lines. We will also present a thiophenecarboxylate like compound that displays favorable cytotoxicity in a leukemia cell line from our ChemBridge DIVERset library.

1.7 Drug discovery

Cytotoxic agents that have been tested on both cancer and non-cancer cell lines have been cytotoxic towards both. Selectivity amongst the compounds are now of interest. Cytotoxic agents that induce cell death are more favorable than those that induce a necrotic death. Cells undergoing a necrotic death cause the recruitment of immune cells and cause the release of pro-inflammatory signals that can provide tumor cells a

microenvironment with beneficial growth factors [21]. Compounds that possess the ability to induce a favorable death, target a variety of mechanisms could be a more effective drug for cancer treatment.

CHAPTER 2: PROJECT INTRODUCTION

Our laboratory has previous published works on piperidone compounds that have been shown to be cytotoxic [20,22]. Here we display, two piperidone compounds, 2608 and 2610, in this study.

Swain RM, Contreras L, Varela-Ramirez A, Hossain M, Das U, Valenzuela CA, et al. Two novel piperidones induce apoptosis and antiproliferative effects on human prostate and lymphoma cancer cell lines. Investigational New Drugs 2022 40:5 [Internet]. Springer; 2022 [cited 2022 Aug 24];40:905–21. Available from: https://link.springer.com/article/10.1007/s10637-022-01266-y

2.1 Introduction

Cancer begins when a cell continues to divide uncontrollably, and all of the daughter cells produced contain the same corrupt replication machinery. At that point, the tumor can either be diagnosed as either malignant or benign. A malignant tumor is defined as an invasive group of cells that can potentially affect nearby tissue and proliferate uncontrollably at another origin in the body, causing cancer in a new area [23]. The overall loss of cell adhesion allows a malignant cell to dissociate from the original tumor into new tissue [24]. This single event results in the death of many individuals with an invasive type of cancer.

Cancer aberrations in cell signaling pathways can manipulate normal progression and division rates in non-cancerous cells, such as signaling for apoptosis, normal-rate division, contact inhibition, and replication machinery. The vast majority of the time, cancer cells inhibit the signals that lead to apoptosis. They do this by either overexpressing antiapoptotic proteins or under the expression of proapoptotic proteins [25]. Those very slight changes can cause intrinsic resistance to current therapies like chemotherapy and prevent the cell from undergoing natural cell death [25].

When cells undergo malignant transformation, they lose the ability to utilize contact inhibition to prevent over proliferation. This transformation gives rise to the malignant cells' ability to invade host tissues for tumor growth, invasion, and ultimately metastasis [26]. With this in mind, this project is aimed to test compounds that may possess anticancer activity. Utilizing other treatment methods, such as a therapeutic approach with compounds that can activate the apoptotic pathway, can be beneficial and need to be further explored. Here we will provide an extensive investigation of therapeutic

piperidone compounds 2608 and 2610. Piperidones have been previously shown to possess anticancer activity[27]. In addition, they have also been known to possess antibacterial [28], antimalarial [29] anti-inflammatory [30], and anti-proliferative activities [31]. Compounds containing a piperidone like structure have been previously reported to induce cell death in leukemia/lymphoma cell lines [32,33]. Thus, acting as proteosome inhibitors and leading to the activation of pro-apoptotic pathways [32,33]. The design of the compounds was based on the considerations of tumors utilizing glycolysis for the production of energy and pyruvate dehydrogenase kinase I (PDK1) in order for glycolysis to occur. The inhibition of the enzyme potentially may diminish tumor development. Dichloroacetic acid is a designated anticancer agent and is known to be an inhibitor of PDK1 [34]. Effort has been made to prepare the analogs containing a 1,5-diaryl-3-oxo-1,4-pentadienyl pharmacophore mounted on the heterocyclic and cycloaliphatic scaffolds [35,36]. These compounds were synthesized via the synthetic chemical route outlined in Fig 1. Leading to the acid-catalyzed condensation between the 4-piperidone and various substituted aryl aldehydes led to the intermediate 3,5-bis(benzylidene)-4-piperidones, which were acylated with dichloroacetyl chloride to give the desired products 2608 and 2610 [33]. Here we explore the two piperidone compounds 2608 and 2610 and their ability to induce reactive oxygen species (ROS) accumulation, depolarization of the mitochondria, activate caspase 3/7, and cause cell-cycle arrest.

2.2 Lab Purpose

Our lab focuses primarily on screening potentially cytotoxic compounds on various cancer cell lines and going above and beyond to determine which mechanism the

compound utilizes to induce cell death. For Chapter 2, We will focus on two novel piperidone compounds, 2608 and 2610, sent from our collaborator Dr. Dimmock from the University of Saskatchewan. The experimental compounds are from a 2000 series library that was synthesized through previously published articles [37]. These analogs will be tested on leukemia/lymphoma and colon cell lines to gauge their variability on different cell lines. For our chapter 3, we will explore a new compound, F8 (methyl 5-[(dimethylamino)carbonyl]-4-methyl-2-[(3-phenyl-2-propynoyl)amino]-3-thiophenecarboxylate), that was discovered in our 30,000 compound library. The compound showed favorable cytotoxicity towards leukemia cell lines. Here we will explore the compounds mechanism of death and phosphorylation inhibition abilities.

2.3 Evaluate the cytotoxicity of compounds 2608 and 2610 on cancer cell lines

Differential nuclear staining (DNS) bioimaging assay to determine CC_{50}

The potential cytotoxicity of the compounds was evaluated on CEM and COLO 205 cell lines and various other cell lines using a live-cell DNS bioimaging assay[38]. Cells were grown and seeded in 96-well plates with a density of 10,000 cells per well in 100 µl of tissue culture medium. Cells were then treated with a concentration gradient (0.1 µM-5 µM) of the two piperidones for a 48 h time point. Both compounds were analyzed in each plate, including a compound solvent control (dimethyl sulfide; 1% DMSO; Millipore Sigma, St. Louis, MO USA), a positive control 1 mM hydrogen peroxide (H_20_2; Millipore Sigma, St. Louis, MO USA), and untreated cells to monitor the background of the dead cell population. To distinguish between the live/dead cell populations, a mixture of propidium iodide (PI; Biotium; Fremont, CA, USA) and Hoechst 33342 (Invitrogen; Eugene, OR, USA), both DNA intercalating fluorescent dyes, was added to each well (5

μg/ml each) 2 h prior to reading and incubated at 37ºC. Hoechst is a fluorescent dye that is permeable to both live and dead cells. In contrast, PI is selective and can only permeate cells whose plasma membrane has been compromised and is used primarily to label the dead cells. Images were captured from each treated well using a multi-well plate reader IN Cell 2000 analyzer (GE Healthcare; Pittsburg, PA, USA). Cytotoxic concentrations of 50% were then obtained using a linear interpolator calculator (https://www.johndcook.com/interpolator.html).

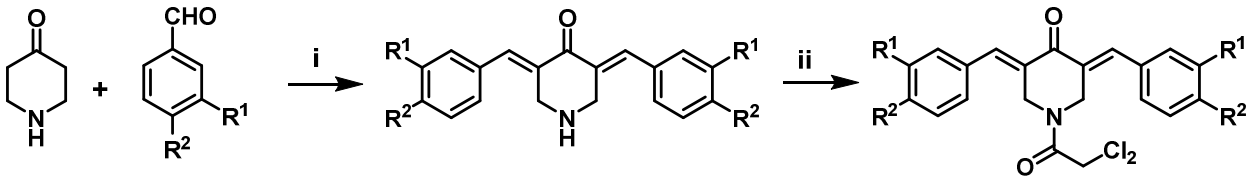

2608 : $R^1 = R^2 = F$

2610 : $R^1 = R^2 = Cl$

Figure 1: Synthesis of 2608 and 2610. i = HCl/CH_3COOH, ii = $Cl_2CHCOCl$. The 2608 (1-dichloroacetyl -3,5-bis(3,4-difluorobenzylidene)-4-piperidone) and 2610 (1-dichloroacetyl-3,5-bis(3,4-dichlorobenzylidene)-4-piperidone) structures are depicted.

The cytotoxic effects of 2608 and 2610 piperidones were analyzed using the DNS imaging assay on twelve human cancer cell lines and two non-cancerous fibroblast cell lines. The DNS assay is reliable and validated for primary and secondary screens for potential anticancer cytotoxic experimental compounds [38,39] [40]. This assay utilizes Hoechst fluorescent dye that permeates both living and dead cells when treated 2 h before reading [41]. In addition, PI stains the nucleus of dead or dying cells with a compromised plasma membrane. As indicated in Table 1, both 2608 and 2610 piperidones display a range of cytotoxicity across various cancer cell lines tested. The cell lines that were grown in suspension, lymphoma, leukemia, and multiple myeloma

cell lines, CEM, RAMOS, U266, RPMI-8226, MM1R, MM1S and HL-60, were incubated for 48 h with 2608 or 2610 to obtain the CC_{50} values. The adherent cell lines, HT-29, MDA-MB-231, PC-3, Hs-27, PANC-1, CCD-112-CoN, COLO 205, and MCF-10A, were initially incubated overnight to allow their attachment to the bottom of the plate, in the absence of the experimental compounds. Next, a concentration gradient of the piperidones was added to the cells and incubated for an additional 48 h, obtaining a dose-response curve to calculate the concentration at which 50 percent (CC_{50}) of the cell population dies. The CC_{50} values ranged from 0.02 μM on CEM to 1.1 μM on PANC-1 cell lines.

Table 1: 2608 and 2610 cytotoxic concentrations 50% (CC_{50}) on various cancer cell lines at a 48 h time point. Selective cytotoxicity index (SCI) values for 2608 and 2610 treated cancer cells are displayed. SCI values were calculated using the following equation: CC_{50} of non-cancer cells divided by the CC_{50} of the cancer cell line. Sci calculated using Hs-27 as non-cancer cell line.

		2608			**2610**		
CELL TYPE	**CELL LINE**	**CC_{50} (μM)**	**S.D.**	**SCI**	**CC_{50} (μM)**	**S.D.**	**SCI**
Acute Lymphoblastic Lymphoma	CEM	0.02	0.003	22.75	0.03	0.004	6.66
Burkitt's Lymphoma	RAMOS	0.095	0.041	4.789	0.036	0.005	5.55
Acute Promyelocytic Leukemia	HL-60	0.064	0.041	7.109	0.024	0.011	8.33

Breast Adenocarcinoma	MDA-MB-231	0.047	0.008	9.68	0.121	0.055	1.65
Breast Epithelial	MCF-10A	0.175	0.007	2.6	0.120	0.004	1.66
Colorectal Adenocarcinoma	HT-29	0.162	0.021	2.80	0.036	0.004	5.55
Colorectal Adenocarcinoma	COLO 205	0.424	0.010	1.07	1.664	0.184	0.12
Colon Fibroblast	CCD-112-CoN	0.12	0.042	-	0.176	0.015	-
Normal Foreskin Epithelial	HS-27	0.455	0.035	-	0.2	0.028	-
Pancreatic Carcinoma	PANC-1	1.132	0.259	0.40	0.4135	0.045	0.48
Prostatic Adenocarcinoma	PC-3	0.301	0.005	1.51	0.446	0.003	0.44
Multiple Myeloma	U266	0.0144	0.001	31.59	0.762	0.010	0.26
Multiple Myeloma	RPMI-8226	0.0397	0.002	11.46	0.3335	0.031	0.599

Multiple Myeloma	MM1 S	0.0181	0.0007	25.138	0.0261	0.0028	7.66
Multiple Myeloma	MM1 R	0.0160	0.001	28.43	0.009	0.005	22.22

Table 1 displays the selectivity of compounds 2608 and 2610 on a range of cancer cell lines. Some CC_{50} values were in the nanomolar range, which is ideal for an anticancer therapeutic agent. As the vast majority of CC_{50} values are below 1 μM range, this gives us further indication of the compounds' toxicity and will pave the way to further experimentation. The following assays were focused primarily on leukemia/lymphoma cell lines and colon cancer cell lines as a comparison since they were the most sensitive and resistant, respectively, to the experimental piperidones. We will be utilizing the 24 h CC_{50} of compounds 2608 and 2610 in the various assays (Table 2.)

2.4 Investigate the cytotoxicity of compounds 2608 and 2610 on leukemia/lymphoma and colon cell lines

The CC_{50} were assessed in CEM and COLO 205 for 24 h in order to obtain 24 h CC_{50}.

Table 2: 24 h CC_{50}'s of compounds 2608 and 2610 with standard deviation calculation.

	2608		2610	
CELL LINE	**CC_{50} (μM)**	**SD**	**CC_{50} (μM)**	**SD**
CEM	0.0993	0.00093	0.0932	0.00098
COLO 205	1.904	0.298	3.791	0.409

2.5 Determine the mechanism of action of 2608 and 2610 on leukemia/lymphoma and colon cell lines

An early indication of apoptotic death is the externalization of phosphatidylserine (PS) on the cellular surface [42,43]. With the use of flow cytometry, PS can easily be detected *via* Annexin V-FITC. CEM cells were seeded in a 24-well plate at 100,000 cell density in 1 mL of media [43]. COLO 205 cells were seeded in the same manner, respectively. The cells were then incubated overnight and treated for 24 h with 2608 and 2610 2X CC_{50}'s. For vehicle control, cells were treated with DMSO; as a positive control of cytotoxicity, cells were treated with 1 mM H_2O_2, and untreated control cells were used to monitor the background of the dead cell population. Cells growing in suspension were then harvested and placed in pre-chilled flow cytometric tubes. Whereas adherent cells were treated with 400 µl trypsin, incubated for 5 min, and collected in flow cytometric tubes. Cells from each well were washed with ice-cold PBS and centrifuged at 1200xRPM for 5 min. Cell pellets were then gently resuspended with annexin V-FITC and PI in 100 µl of binding buffer and incubated in the dark for 15 min on ice. Prior to analyses by flow cytometry, cells were added with 400 µl of ice-cold binding buffer. Approximately 10,000 events/cells were acquired per individual sample by using Kaluza software (Beckman Coulter). The total apoptotic cell populations are depicted as the sum of both early and late facets of apoptosis. Three independent measurements were performed, and the average and standard deviation were calculated, obtaining the percentage of both apoptotic and necrotic cells.

Phosphatidylserine Externalization

To determine whether both 2608 and 2610 cause cell death *via* apoptosis or necrosis, we measured the externalization of phosphatidylserine (PS) in CEM and COLO 205

cells, respectively, using an annexin-V-FITC/PI assay. For this assay, we used the 2X CC_{50} concentrations determined on CEM and COLO 205 for both 2608 and 2610 (see Fig.2 for details). The data indicate significant PS externalization compared to the DMSO solvent control for both cell lines. As expected, a high percentage of PS externalization was detected when cells were treated with the positive control H_20_2 (39%), whereas DMSO and untreated cells showed low PS externalization (18-19%). Furthermore, the results indicate that both compounds triggered apoptosis's mechanism to induce cell death due to the significant percentage of PS externalization in CEM and COLO 205. However, PS externalization was more pronounced in the CEM cell line.

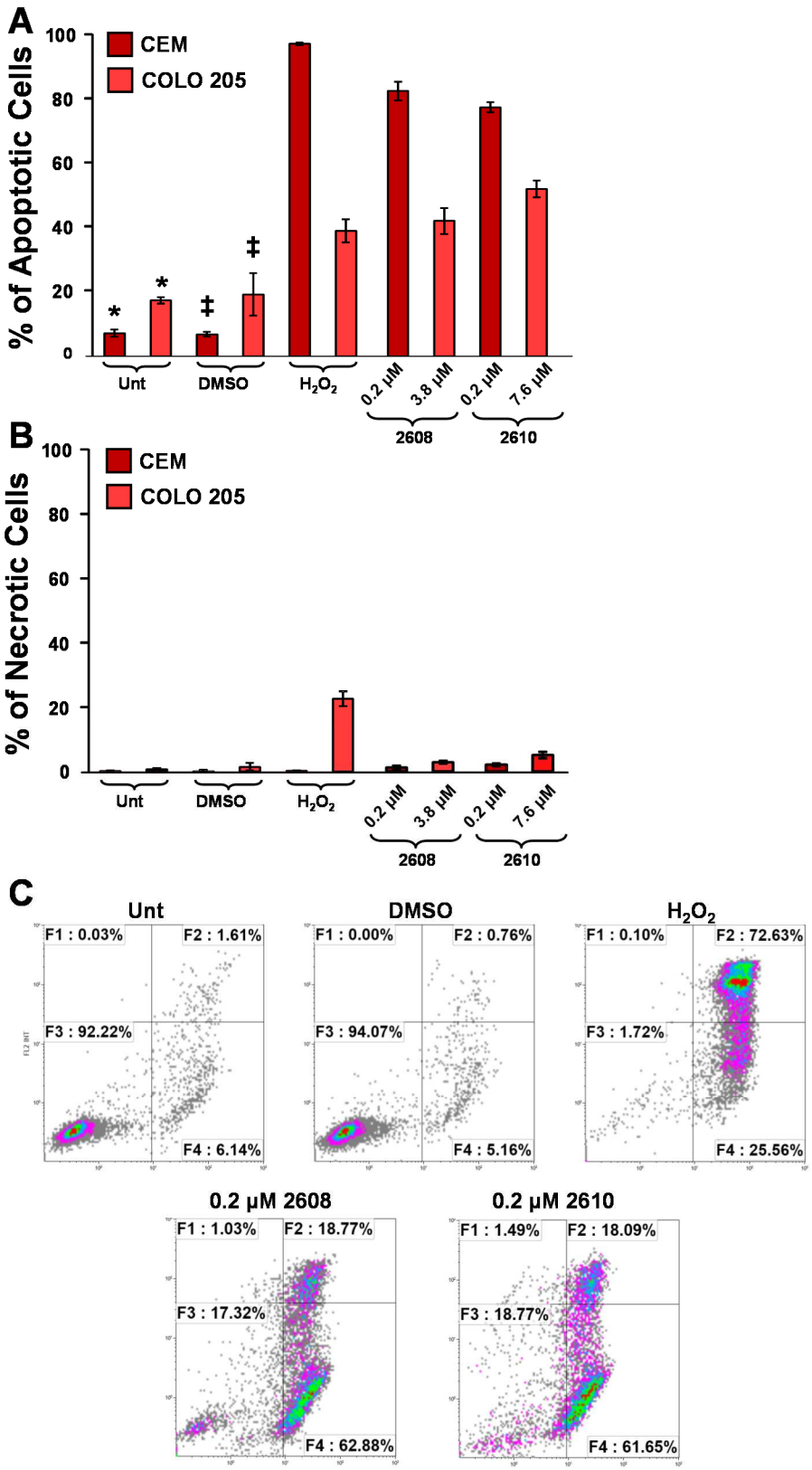
A
% of Apoptotic Cells
CEM
COLO 205
Unt
DMSO
H2O2
0.2 µM
3.8 µM
0.2 µM
7.6 µM
2608
2610
B
% of Necrotic Cells
C
Unt
F1 : 0.03%
F2 : 1.61%
F3 : 92.22%
F4 : 6.14%
DMSO
F1 : 0.00%
F2 : 0.76%
F3 : 94.07%
F4 : 5.16%
H2O2
F1 : 0.10%
F2 : 72.63%
F3 : 1.72%
F4 : 25.56%
0.2 µM 2608
F1 : 1.03%
F2 : 18.77%
F3 : 17.32%
F4 : 62.88%
0.2 µM 2610
F1 : 1.49%
F2 : 18.09%
F3 : 18.77%
F4 : 61.65%

Figure 2. Both experimental piperidones induce significant PS externalization in CEM and COLO 205 cells in a dose-dependent modality. Cells were exposed to the experimental piperidones for 24 h, and cells were then stained with Annexin V and PI and monitored via flow cytometry. Fig 2A and 2B contain % of apoptotic cells that are Annexin V-FITC positive, whereas panel 2b shows % of necrotic cells that are PI-positive Annexin V-FITC negative. The following controls were included: DMSO as solvent control, 1 mM H2O2 was incorporated as a positive control for cytotoxicity, and untreated (Unt) cells. Statistical analyses were accomplished using a two-tailed Student's paired t-test. The asterisk (*) annotations compare untreated cells with 2X CC_{50} of both 2608- and 2610-treated cells with P-values of <0.00001 and 0.00001 for CEM and P-values of <0.007 and 0.0001 for COLO 205, respectively. The double dagger symbols (‡) compare the DMSO-treated cells with CC_{50} of 2608- and 2610-treated cells with P-values of <0.00001 and 0.00001 for CEM and P-values of <0.0005 and 0.00003 for COLO 205, respectively. Representative flow cytometric dot plots were used in panel C to create the bar graphs corresponding to CEM cells.

Analysis of mitochondrial membrane potential using JC-1 and flow cytometry

CEM and COLO 205 cells were seeded in 24-well plates and treated with 2608 and 2610 2X CC_{50} for an 8 h incubation. Following treatment, the cells were harvested and labeled with fluorophore 5,5,6,6-tetraethylbenzimidazolylcarbocyanine iodide (JC-1). A flow cytometer was used to capture the cells' red and green signals. Healthy cells with polarized mitochondria will emit a red fluorescence signal due to the JC-1 aggregated formation [39,42]. In contrast, once the mitochondria are depolarized, they will form JC-1 monomers exhibiting a green fluorescence signal. The controls used in this series of experiments were similar to those in the above assay. Each data point represents the average of at least three independent measurements.

High ROS production levels are known to lead to mitochondrial depolarization, including damage of DNA, proteins, and lipids [44] [45]. To further investigate the mechanism by which 2608 and 2610 induce cell death, we evaluated both compounds in CEM and COLO 205 cells using the JC-1 polychromatic fluorescent reagent and flow cytometry. Both CEM and COLO 205 cells were incubated for 6 h with the compounds, and the mitochondrial membrane potential was examined. This analysis revealed that the

piperidones induced significant mitochondrial depolarization at twice the CC_{50} concentration compared to the untreated and DMSO-treated cells for CEM and COLO 205 (Fig. 3). Overall, these findings further confirm that compounds 2608 and 2610 are able to depolarize the mitochondria, indicating that the compounds induce apoptotic death.

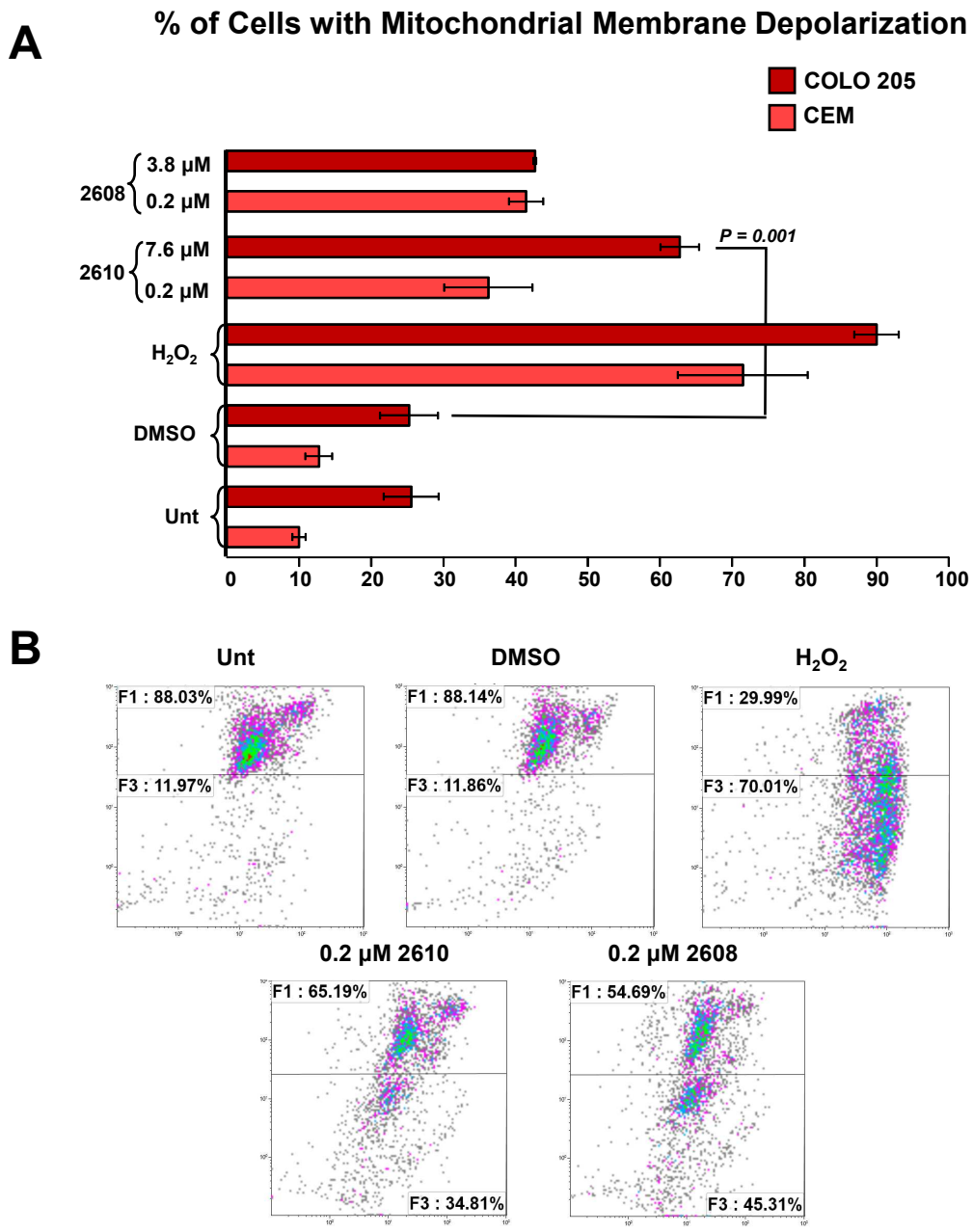

Figure 3. The experimental piperidones induced significant mitochondrial depolarization activity on COLO 205 and CEM cells. Cells were incubated for 6 h with the experimental piperidones and then stained with JC-1 reagent and monitored by flow cytometry. Statistical analyses were acquired by using the two-tailed Student's paired t-test. The asterisk annotations on each bar graph represent the statistical significance of the experimental treatments compared with the vehicle control (1% DMSO). Cells treated with 1 mM H_2O_2 were included as an inducer for mitochondrial depolarization. Representative flow cytometric dot plots were used in panel B to create the bar graphs corresponding to CEM cells.

Piperidone compounds induce an accumulation of Reactive Oxygen Species (ROS)

The production of ROS signals for oxidative damage in the mitochondria by retrograde redox signaling was investigated [46]. Analysis of ROS production in CEM and COLO 205 cells treated with 2608 and 2610 24 h 2X CC50 was conducted via carboxy-H2 DCFDA (6-carboxy-2' 7'dichlorodihydrofluorescein diacetate) fluorescein reagent (Invitrogen, C400) and analyzed by flow cytometry. CEM and COLO 205 cells were seeded in a 24-well plate at a density of 100,000 cells per well in 1mL of culture medium. CEM and COLO 205 cells were treated with compounds 2608 and 2610 8 h prior to reading. The controls mentioned above were used for this experiment, as well. Cells were collected and placed in flow cytometry tubes and centrifuged for 5 min at 1200 RPM. Cells were gently resuspended in PBS containing carboxy-H2 DCFDA (master mix/loading buffer) and incubated for 1 h. Cells were then centrifuged again to remove the excess loading buffer and resuspended in 500 µl of fresh PBS. Immediately after, cells were analyzed *via* flow cytometry, acquiring ~10,000 events (cells) per sample. Cytometry analysis was performed as in the previous section.

To further examine the mechanism by which 2608 and 2610 induce cell death, the accumulation of ROS in CEM and COLO 205 cells was measured after treatment of cells with the piperidones for 6 h with 24 h 2X CC_{50}. We incubated for 6 h in order to detect ROS generation. A longer incubation time would not have been advantageous; as ROS generation occurs in the early stages of apoptosis [47]. Following the exposure to the 24 h 2X CC_{50} for both compounds, the cells were incubated for one hour with 10 µM of carboxy-H2 DCFDA ROS. Subsequently, the cells were analyzed *via* flow cytometry for those emitting a green signal indicating ROS accumulation. As shown in

Fig.3, both CEM and COLO 205 cells generated ROS in the presence of the 2X CC_{50} of 2608 and 2610, indicating the induction of the intrinsic apoptotic pathway. However, the accumulation of ROS was more prominent in the CEM cell line than in COLO 205.

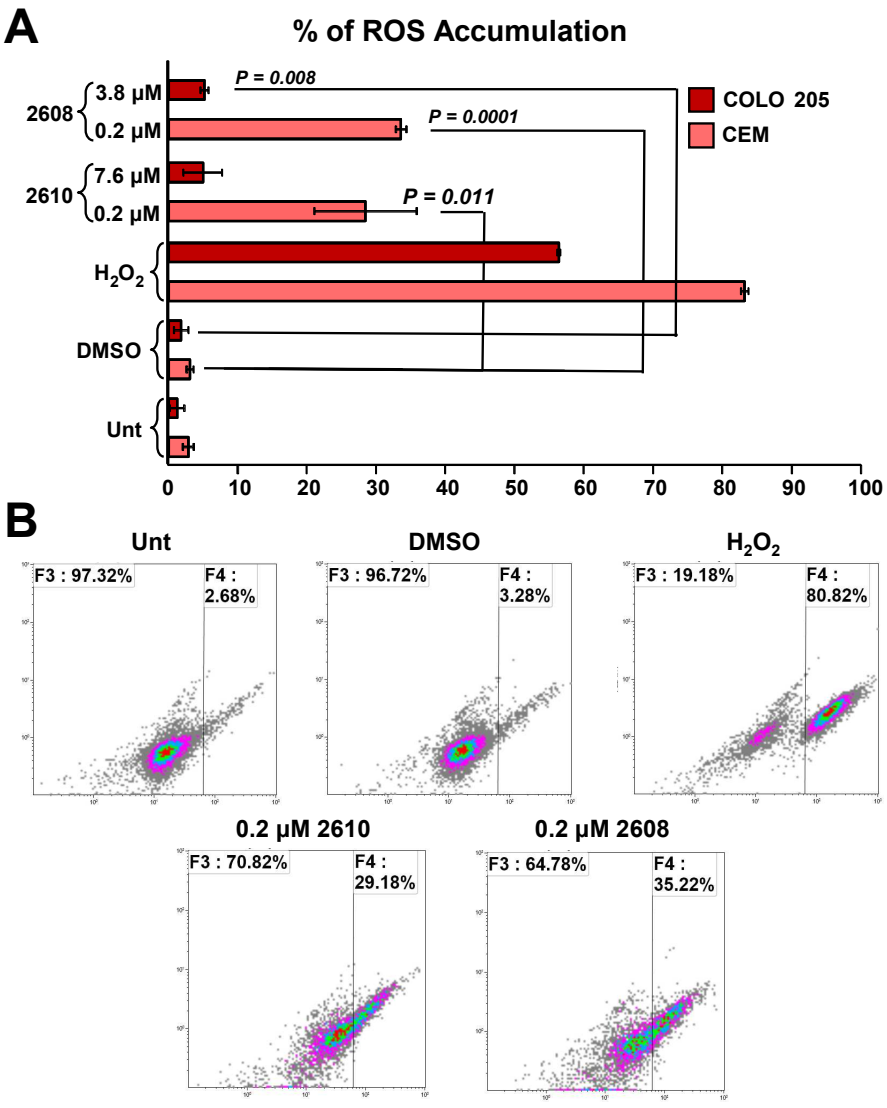

*Figure 4: Significant ROS induced by 2610 and 2608 piperidones on CEM cells and COLO 205, as compared with the DMSO-treated cells. Statistical analyses were acquired by using the two-tailed Student's paired t-*test. *H_2O_2 (1 mM)-treated cells were*

included as an oxidative stress positive control. Representative flow cytometric dot plots were used in panel B to create the bar graphs corresponding to CEM cells.

Caspase 3/7 Activation

The cellular activation of caspase 3/7 was detected by adding the cell membrane-permeable fluorogenic NucView 488 caspase 3/7 substrate [48]. This substrate can permeate living cells with an intact plasma membrane and allow for identifying active caspase 3/7. The cells were examined *via* flow cytometry with the same plating methodology, as previously mentioned [43] and treated with their 24 h 2X CC_{50} respectively (CEM 2608 2X CC_{50} 0.1986 µM and 2610 2X CC_{50} 0.1864 µM and COLO 205 2608 2X CC_{50} 3.808 µM and 2610 2X CC_{50} 7.582 µM). Cells were harvested in flow cytometry tubes and centrifuged at 1200 RPM for 5 min. Cell pellets were gently resuspended in 200 µl of PBS, containing 5 µl of NucView488 caspase 3/7 substrate, and incubated in the dark for 45 min at room temperature. After this step, 300 µl of PBS was added to each flow cytometry tube. A green fluorescent signal indicated caspase 3/7 activation within the cell during the analysis. Furthermore, 10,000 events were assessed per sample. Each sample was performed at least three times. For sample acquisition and analysis purposes, the Kaluza software was utilized (Beckman Coulter).

It is known that the activation of caspase-3/7 is a biological marker of a cell undergoing apoptosis [49]. Individual caspases mediate apoptosis and various other biological processes [49]. In this study, we analyzed the activation of caspase-3/7 *via* flow cytometry by using a live-cell NucView 488 caspase-3/7 fluorogenic enzyme substrate after 7.5 hours of incubation of CEM and COLO 205 cells with both piperidones. As shown in Figure 5, a significant amount of caspase-3/7 activation was detected at twice

the CC_{50} concentrations of both compounds compared to the untreated and vehicle control cells. For the positive control, H_2O_2-treated cells were significant for caspase-3/7 activation (Figure 5). These results showed that compounds 2608 and 2610 induce cell death through the caspase-3/7 activation pathway for both cell lines, a hallmark of apoptosis.

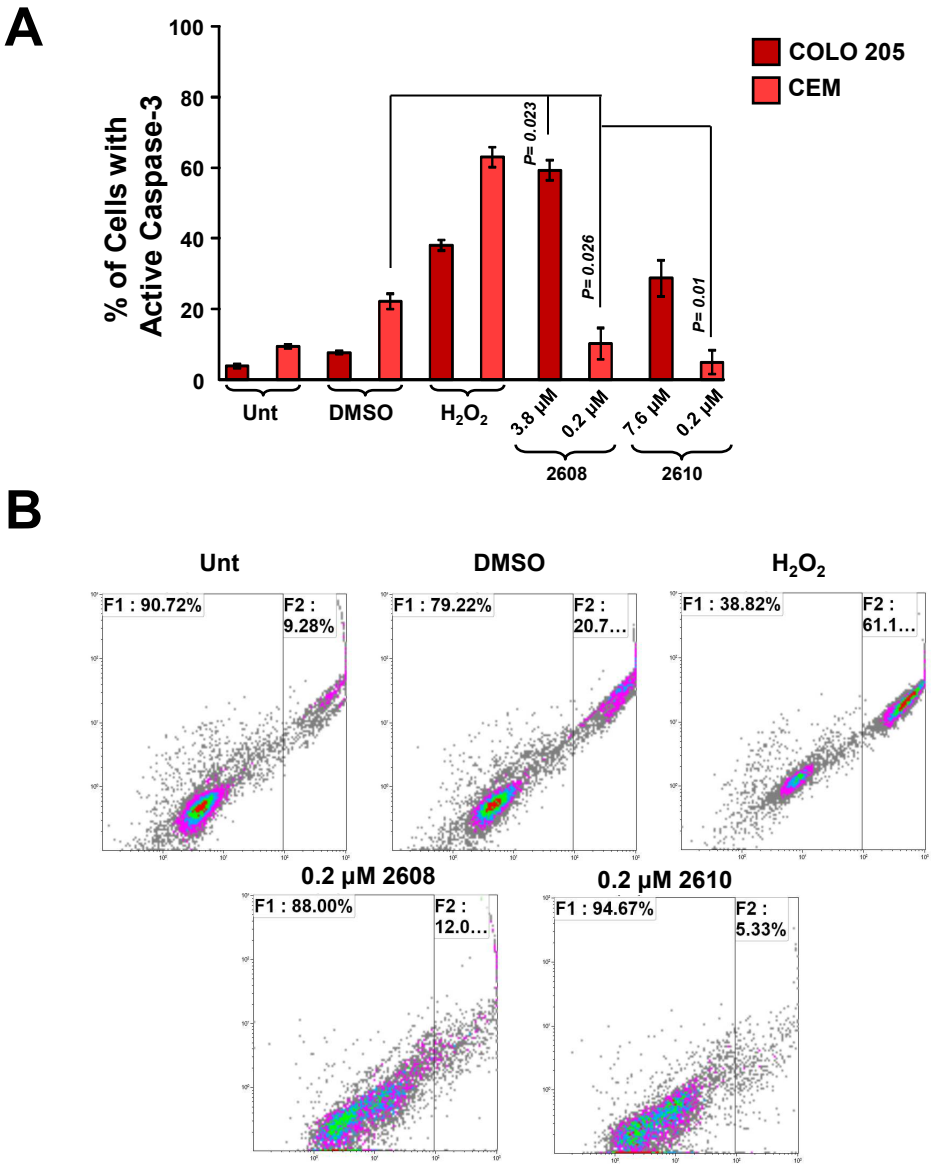

Figure 5. Both 2610 and 2608 piperidones induce significant caspase-3/7 activation in COLO 205 and CEM cells. Cells were incubated for 7.5 h with the piperidones, stained with NucView 488 caspase 3/7 substrate, and analyzed via flow cytometer.

Statistical analyses were obtained by using the two-tailed Student's paired t-test. The statistical significance of the experimental treatments compared with the vehicle control (1% DMSO). Cells treated with 1 mM H_2O_2 were included as a caspase-3/7 activator control. Representative flow cytometric dot plots were used in panel B to create the bar graphs corresponding to CEM cells.

Cell cycle profile analysis via flow cytometry

To investigate the mechanism at which the compound induces cell arrest, CEM and COLO 205 cells were seeded in 24-well plates at a density of 100,000 cells per well in 1 ml of media [50]. CEM cells were treated with 2608 CC_{20} (0.0397 μM) and 2610 CC_{20} (0.0372 μM), and incubated for 72 h. COLO 205 cells were treated with 2608 CC_{20} (0.7616 μM) and 2610 CC_{20} (1.5164 μM) and incubated for 72 h. The controls used for these experiments were the same as described above. Following incubation, cells were collected in flow cytometric tubes, centrifuged at 1200 RPM for 5 min, and resuspended in 100 μl of room temperature media. Lastly, a single nuclear isolation medium (NIM)-DAPI reagent was added to each flow cytometry tube (200 μl) and analyzed *via* flow cytometry [39,51]. This dye is able to stain the cell nuclei facilitating the quantification of the total amount of DNA per cell. Roughly 10,000 events/cells were acquired per sample (Gallios; Kaluza software; Beckman Coulter). For this purpose, the FL-9 detector and 405 nm laser were solely responsible for quantifying the total DNA content for each event (cell) and distributing them to the designated subpopulation. Each experimental point and its corresponding controls were performed using at least three independent measurements.

A cell cycle analysis was conducted in order to determine if compounds 2608 and 2610 induce cell cycle alterations and ultimately cause the arrest and antiproliferative cellular activity. The cell cycle profile was examined *via* flow cytometry utilizing the DNA intercalating agent, DAPI (4',6-diamidino-2-phenylindole). Both CEM and COLO 205

cells were treated with a low concentration of 2608 or 2610 (CC_{20} concentrations) and incubated for 72 h. It is important to note that at the CC_{50} concentrations of both compounds, extensive DNA degradation was observed in both cell lines that interfered with the cell cycle analyses (data not shown). Low concentrations of compound (CC_{20}) were used to monitor the cell cycle phase levels. As in those presented in the other sections, the same controls were used in this experimental series. After incubation, both 2608 and 2610 did not alter the cell cycle profile in the cell lines tested, CEM and COLO 205 (Figure 6). Given the data, 2608 induced DNA fragmentation in CEM cells but not in COLO 205. In comparison, 2610 caused DNA fragmentation on both cell lines, CEM and COLO 205 (Figure 6A). The *P*-values of DMSO-treated CEM cells compared with 2608 and 2010 treated CEM cells were 0.0036 and 0.011, respectively. The *P*-value of COLO 205 DMSO treated cells compared with 2608 treated COLO 205 cells was insignificant, whereas when compared with 2610 treated COLO 205 cells was 0.0038. Thus, the DNA fragmentation activity of 2608 was selective on CEM cells, whereas 2610 exhibited this activity on both cell lines tested. Also, both 2608 and 2610 compounds did not induce arrest in any cell cycle facets.

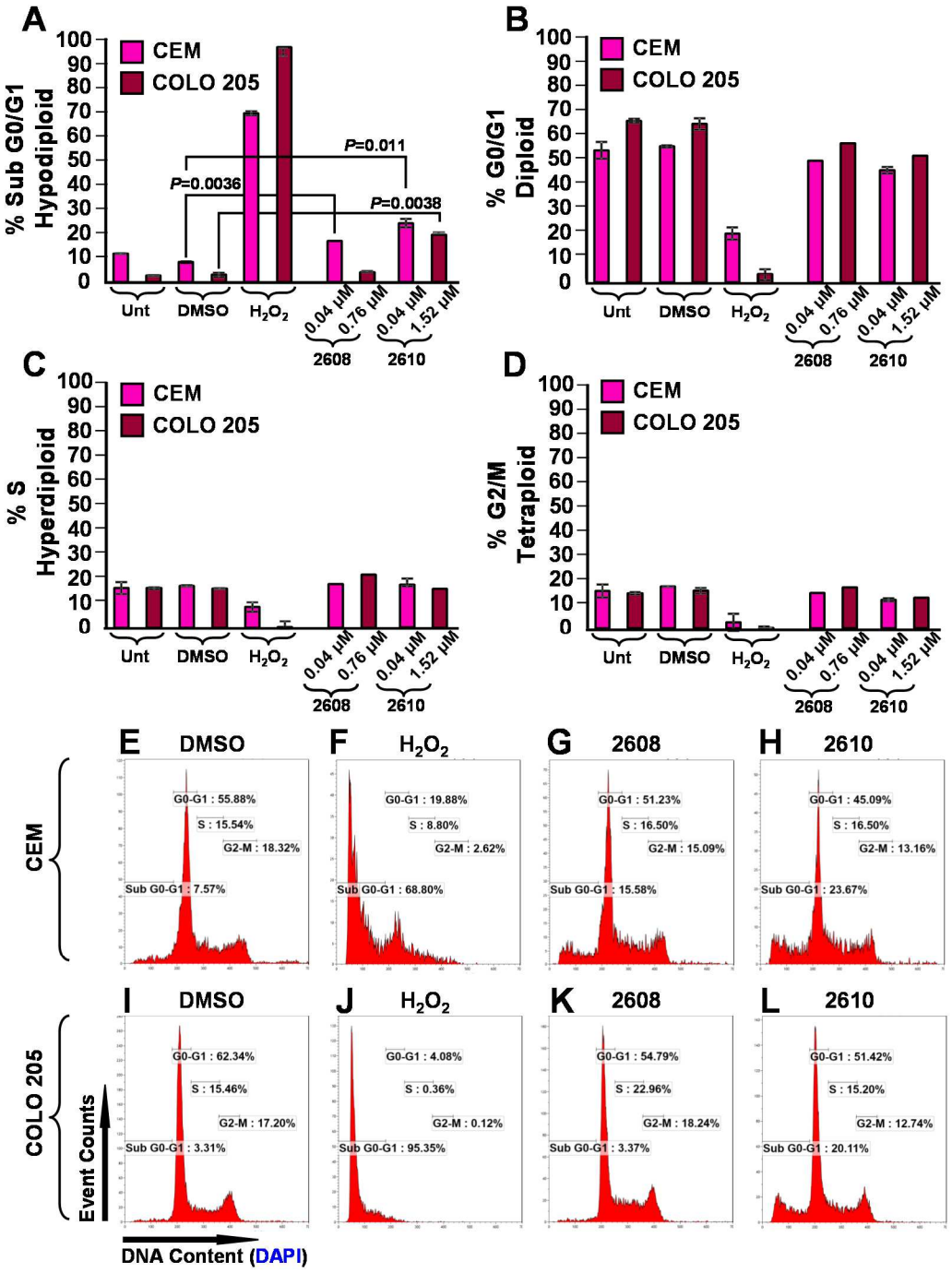

*Figure 6. 2608 elicited selective DNA fragmentation on just CEM cells, and 2610 induced significant DNA fragmentation on CEM and COLO 205 cells (**A**; sub G0/G1), without arresting them in a particular cell cycle phase (**B**, **C**, and **D**). The P-values of DMSO-treated CEM cells compared with 2608 and 2010-treated CEM cells were 0.0036 and 0.011, respectively. The P-value of DMSO-treated COLO 205 cells compared to 2610 treated COLO 205 cells was 0.0038. Each bar denotes an average of three independent measurements, and the error bars*

2.6 Investigate compounds 2608 and 2610 Proteasome inhibition

Analysis of poly-ubiquitinated protein in CEM and COLO 205

A total of 3,000,000 CEM and COLO 205 cells were seeded in T-25 flasks in 10 ml of complete RPMI medium. Cells were then treated with 10 µl of the 2x CC_{50} of CEM (0.198 uM) and COLO 205 (3.808uM) 2608, 2610 (CEM; 0.186 uM, COLO 205; 7.582 uM), MG-132, and the vehicle PEG-400 (0.3%) at an 8-hour time period. Following incubation, the cells were then harvested in 15 ml conical tubes to form pellets and transferred to 1.5 ml tubes. The cells were then washed once with 1 ml PBS and pelleted at 1000 g for 6 min. Once pelleted, the PBS was removed, and the pellet was resuspended in 70 µl 2x Laemmli buffer (120 mM Tris-HCl, 0.1% β-mercaptoethanol, 4% SDS, 20% glycerol, and 0.02% bromophenol blue) and boiled at 100 C for 15 min to lyse the cells. Protein was then quantified utilizing a Nano-Drop N-1000 system, and a total of 100 µg per sample was calculated. The final volume of 25 µl was loaded per lane on a 7% SDS PAGE gel and separated at 100V for 1.5 h. The gel was then transferred to a PVDF membrane at 100V for 1 h. Afterward, the PVDF membrane was blocked overnight at 4 C in 5% powdered milk. Following the overnight incubation, the primary antibody, mouse monoclonal anti-Ubiquitin (Santa Cruz Biotech; sc-8017) was added to the membrane and incubated for 1 h. The membranes were washed with TBS-T 3 times for 15 min. The secondary polyclonal goat anti-mouse antibody (1:10,000 diluted in TBS-T) conjugated to horseradish peroxidase (Thermo Fisher; 31,430) was added and incubated at room temperature for 1 h. The membrane was then rewashed with TBS-T 3 times for 15 min to wash away any unbound antibodies. Prior to the reading, the membrane was placed in the iBright machine and labeled with Enhanced

Chemiluminescence Solution (ECL), one part being 1 mL peroxide and 1mL of luminol. The ECL is based on the antibodies that are conjugated to the membrane or labeled with horseradish peroxidase [52]. The addition of the luminol produces excited intermediates, and upon release, it emits a blue signal [52]. Following the wash, the membrane was then read with the Invitrogen iBright Imaging Systems and quantified for further analysis.

In prior reports, several piperidones have been found to disrupt proteasome activity leading to the induction of proteotoxic stress and apoptosis [53]. Proteosome inhibitors have been investigated due to their selective toxicity on cancer cells[54]. The disruption has been previously shown to result in an accumulation of polyubiquitinated proteins and inhibition of proteasomal activity [53]. The accumulation of polyubiquitinated proteins with compounds 2608 and 2610 were evaluated by western blotting after an 8 h treatment. Following densitometric quantification of high molecular weight poly-ubiquitinated proteins, the results denoted a strong increase in polyubiquitinated protein accumulation for compound 2610 in COLO 205 (1.41-fold increase), closely similar to the increase seen in MG132 proteasome inhibitor control (1-fold increase). However, only a slight 0.61-fold increase was observed in CEM cells for this compound. Compound 2608 also showed a moderate increase in the accumulation of polyubiquitinated proteins in COLO 205 and CEM; 0.40- and 0.59-fold increase, respectively (Figure 7).

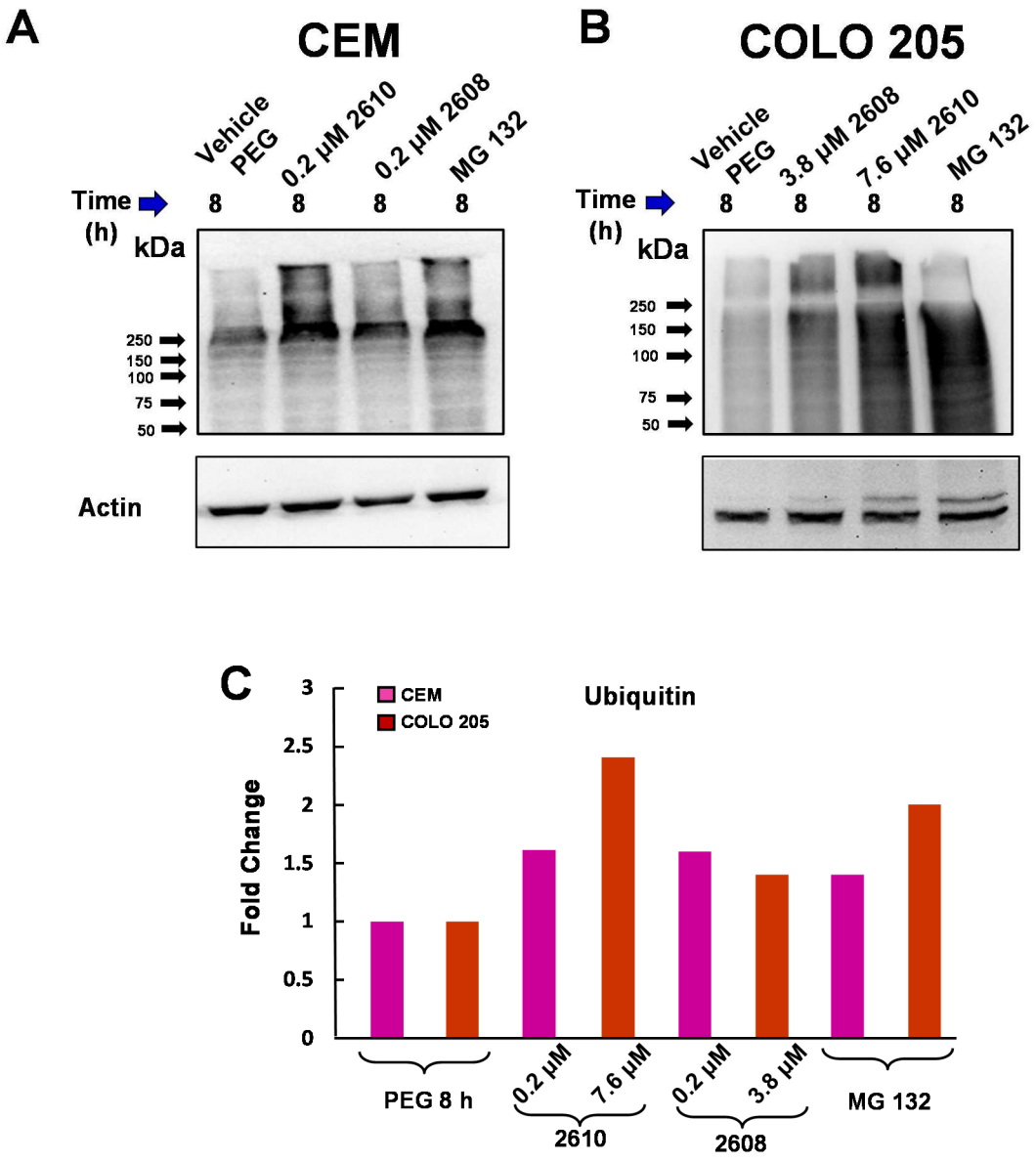

Figure 7. Western Blot analysis reveals an accumulation of high molecular-weight poly-ubiquitinated proteins for both COLO 205 and CEM cell lines. Cells were treated for 8 h time point with; PEG 400 (vehicle control), MG 132 (positive control for proteasomal inhibition), and compounds 2610 and 2608 at a 2X CC_{50} concentration. Panel A indicates western blot analysis performed in CEM cells treated with 2610 and 2608, whereas Panel B shows analysis in COLO 205 cells with compounds 2610 and 2608. Panel C quantifies high molecular weight poly-ubiquitinated proteins (above 50 kDa) by densitometry. Fold change values for both CEM and COLO 205 are displayed.

2.7 Computational Docking

The initial docking was performed utilizing the Schrödinger software suite (Schrödinger, LLC, New York, NY, USA). The protein crystal structure was used for this docking experiment utilizing the protein data bank (https://www.rcsb.org/). The protein targets used for these experiments were UCH-L5 (PDB: 3IHR) and USP14 (2AYO) and were prepared as previously described [55]. Using the Maestro 12.8 interface and Protein Preparation Wizard, the crystalized 3-dimensional figures were prepared. The program was left to run as default, and the options for missing side chains, missing loops, the removal of water, and any other interfering ligands were the only ones selected. Prior to docking, the compounds were optimized and then minimized to expose hidden crystal structures using the Schrödinger Release 2018: LigPrep, Schrödinger, LLC, New York, NY, 2018 interface of the Schrodinger software, with Optimized Potentials for Liquid Simulations 4 force field, at a pH 7 ± 2 using Schrödinger Release 2018: Epik, Schrödinger, LLC, New York, NY, 2018 (OPLS4 force field) [56]. Specific Residues that have been previously identified to form the binding pocket of b-AP15 were used for the receptor grid generation utilizing Schrödinger Release 2021-3: Induced Fit Docking protocol; Glide, Schrödinger, LLC, New York, NY, 2021; Prime, Schrödinger, LLC, New York, NY, 2021 [56]. This generates a binding grid around amino acids Asn85, Cys88, Ala162, and Leu181 for UCH-L5, and Asn109, Cys114, Ser433, Ser432, and Gly434 for USP14. Lastly, molecular mechanics (MM-GBSA) of the docked compounds was performed using the Prime tool on Maestro 12.8 **Schrödinger Release 2018:** Prime, Schrödinger, LLC, New York, NY, 2018, and the best scoring compounds were selected.

Computational Docking of UCHL5

In previously published work, a structure relationship study was performed on piperidone b-AP15 (VLX1500) revealed that this compound acted as a proteasome inhibitor, specifically interacting with Deubiquitinases (DUBs) Ubiquitin-Specific Protease 14 (USP14) and Ubiquitin C-terminal Hydrolase L5 (UCHL5) [56]. USP14 and UCHL5 and two cysteine proteases constitute the deubiquitinating enzymes within the 19S regulatory particle in proteasome 26S [57–60]. The 26S proteasome contains one or two 19S regulatory particles necessary for substrate recognition, deubiquitination, unfolding, and translocation [61,62]. Based on the similar chemical structure of our compounds to piperidone b-AP15, we attempted to determine if they could also interact with USP14 and UCHL5. Utilizing the b-AP15 docking site and PDB code 3IHR, which has been used to generate the grid for docking, we performed *in silico* docking to this site with compounds 2608 and 2610 [56]. The binding affinity b-AP15 to the pocket of UCH-L5 was compared to the potential binding affinities of 2608 and 2610. To expose the hidden pocket in the crystal structure of b-AP15 (PDB: 3IHR), we utilized induced-fit docking to reveal and expose the binding site [56]. The analogs previously described share an α, β- unsaturated carbonyl group that is likely to react with the Cys88 found in said hidden binding pocket [56]. Our docking results confirm the previous experiment with the α, β- unsaturated carbonyl group (Michael acceptors) in proximity with Cys88 [56]. This docking would likely result in covalent binding, making the irreversible molecules inhibitors of UCHL5. With this in mind, compounds 2608 and 2610 lacked α, β- unsaturated carbonyl group, which resulted in a different binding mode and scored higher than b-AP15. Molecular mechanics were then used to approximate the binding

affinity between the protein and the ligand of b-AP15, 2608, and 2610 to UCHL5, resulting in high scores relative to b-AP15, as seen in Figure 8. Both compounds MM/GSA scores 2608 (-68.34 kcal/mol) and 2610 (-73.27 kcal/mol) fell well within the binding score of b-AP15 (-69.25 kcal/mol), indicating that both compounds are likely inhibitors of UCHL5 and bind with relatively good affinity. These results suggest that, like b-AP15, both compounds cause proteasome inhibition.

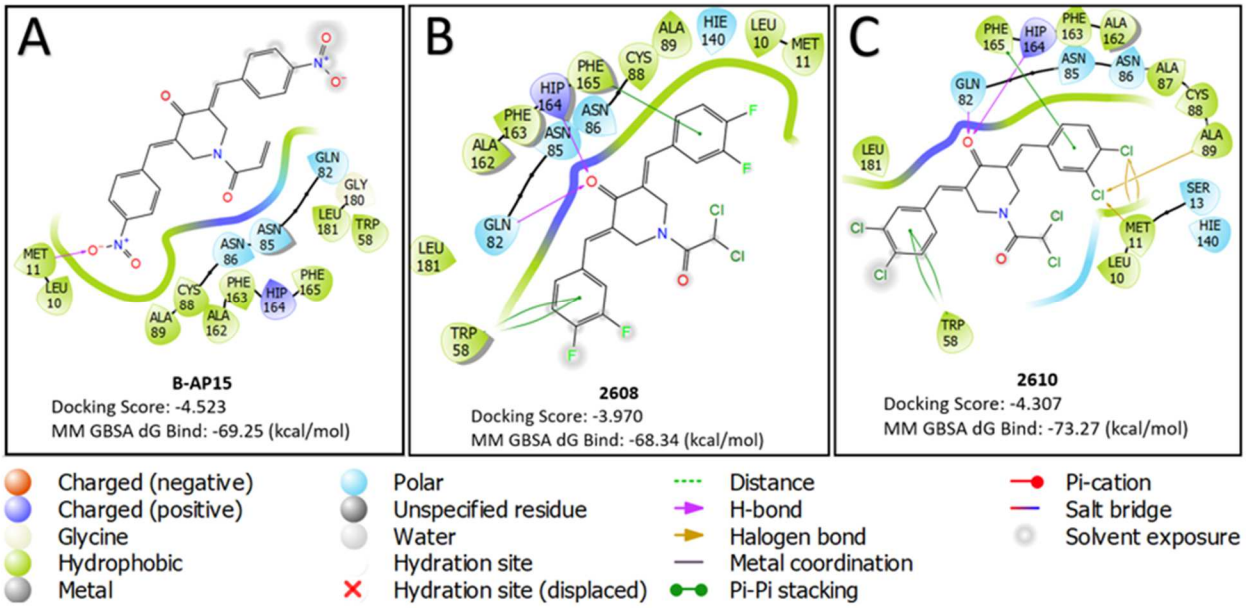

Figure 8. Computational docking of b-AP15 (A), 2608 (B), and 2610 (C) to UCHL5. Exhibited docking scores of, 2608 (-68.34 kcal/mol) and 2610 (-73.27 kcal/mol). Both compounds fell within the score of b-AP15, -69.25 kcal/mol, indicating potential inhibition of UCHL5.

Computational docking of USP14

USP14 plays an essential role in proteasomal degradation [63]. The USP14 has been used to inhibit proteasomal function inducing apoptotic cell death in cancers [63]. As stated above, we utilized USP14 and UCHL5 to compare the docking scores of b-AP15 to our piperidones 2608 and 2610 to observe similarities. The compounds were docked using the same methodology described above with PDB code 2AYO. The best scoring poses of b-AP15 were chosen and used for molecular dynamics (MM-GBSA), which resulted in the binding affinity of -50.76 kcal/mol [56]. The binding affinity of 2608 and 2610 was estimated to be -53.82 kcal/mol and -56.10 kcal/mol, respectively. These results suggest that both can function similarly to b-AP15 inhibiting USP14 function and blocking access to the c-terminus of ubiquitin (25).

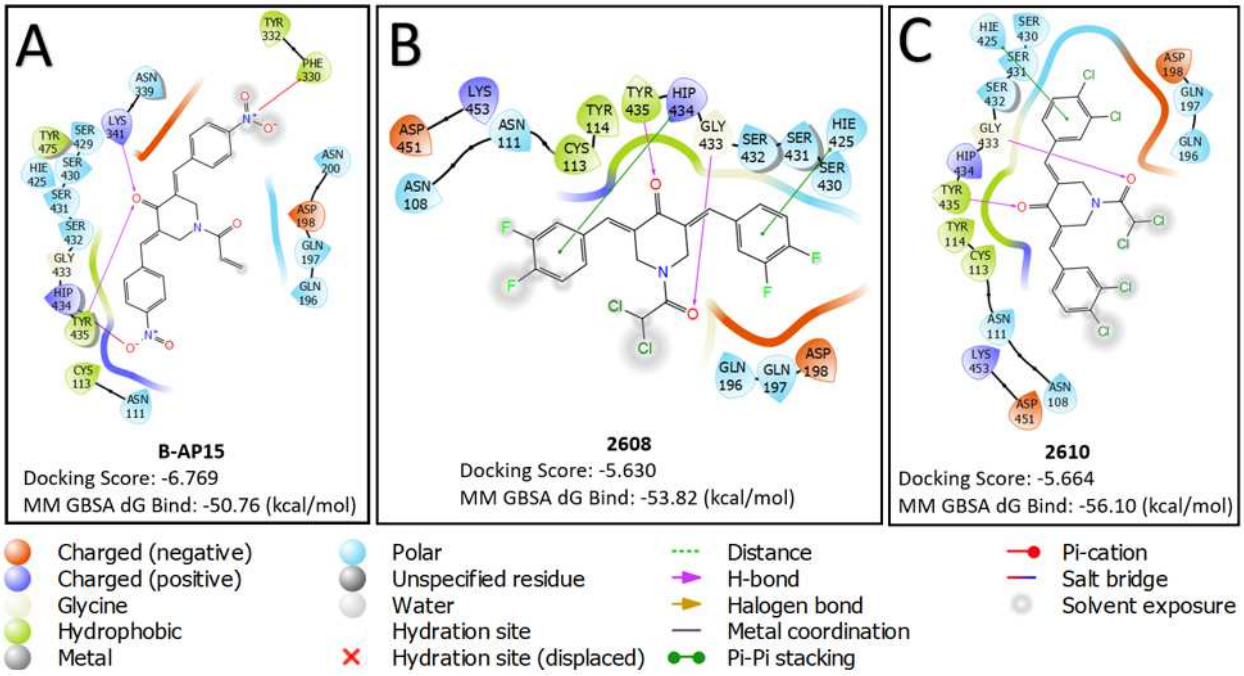

Figure 9. Computational docking of b-AP15 (A), 2608 (B), and 2610 (C) to USP14. Exhibited docking scores of, 2608 (-53.82 kcal/mol) and 2610 (-56.10 kcal/mol). Both compounds fell within the score of b-AP15, -50.76 kcal/mol, indicating potential inhibition of UCHL5 and USP14.

2.8 Chapter 2 Discussion

Previously, it has been shown that piperidone compounds have been highly cytotoxic toward various cancer cell lines [64]. In addition, previous published piperidones, P3, P4, and P5 have demonstrated cytotoxic effects towards tumorigenic cells, as opposed to non-cancerous cells, at the low micromolar range[22]. The treatment of the compounds induced apoptosis via the intrinsic apoptotic pathway and the accumulation of poly-ubiquitinated proteins and the pro-apoptotic protein Noxa [22]. This study demonstrated that both 2608 and 2610 piperidone compounds exhibited cytotoxic activity on 14 different cancer cell lines, ranging from hematological cancers to solid tumors, with CC_{50} values fluctuating from nanomolar to low micromolar concentrations (0.009 μM to 1.664 μM). Compounds P3, P4, and P5 demonstrated less cytotoxicity in CEM and COLO 205 with CC_{50} values ranging from 0.65 μM -0.87 μM for CEM and 0.80 μM -4.66 μM for COLO 205 [22]. Additionally, we examined the effects of the compounds on a non-cancerous cell line and denoted SCI values (Table 1). Of the two compounds, 2608 displayed the highest selectivity (SCI above 5) in most cell lines compared to 2610. For these assays, we utilized a cell line that was most sensitive to the compounds, CEM, and one that is most resistant, COLO 205, to determine if the compounds elicited different responses that may display their resistance or sensitivity to the compounds. Once treated with a cytotoxic compound, cells can undergo apoptosis or necrosis as a cell death mechanism [65]. Thus, we investigated the piperidone compounds cell death mechanism. Hallmarks for apoptosis include the externalization of phosphatidylserine, mitochondrial membrane depolarization, reactive oxygen species generation, and the activation of executioner caspase-3 [66]. After conducting the Annexin V/PI assay, it was determined that both 2608 and 2610 induce cell death *via*

the apoptotic pathway due to the significant PS externalization in both cell lines. In cells undergoing programmed cell death, phosphatidylserine translocates to the outside of the cell membrane and is characteristic of apoptosis [41,42].

When a cell undergoes apoptosis, it can go through the intrinsic or the extrinsic cell death pathway [67]. The intrinsic pathway implicates releasing factors by the mitochondria within the cell [68]. Caspase-3 is also activated by the permeabilization of the outer mitochondrial membrane and by releasing apoptogenic proteins that signal cell death [68]. On the other hand, the extrinsic pathway initiates apoptosis through cell membrane proteins known as death receptors [67]. A mitochondrial depolarization (JC-1) assay was conducted to investigate the depolarization of the mitochondria, which usually occurs when the cell is undergoing apoptosis *via* the intrinsic pathway. Both compounds induced significant mitochondrial depolarization for both cell lines. This depolarization was more prominent in the CEM cell line, proving that the compounds act via the intrinsic apoptotic pathway, as shown in Fig. 4.

To further investigate and characterize the mechanism by which 2608 and 2610 induce cell death, we studied ROS generation after compound treatment of CEM and COLO 205 cells. The generation of ROS plays a role in the intrinsic apoptotic cascade by being released after the mitochondria's membrane is depolarized [47,69] It is well known that the overproduction of ROS can cause cellular stress, activate caspases, and lead to the induction of cell death [66,70]. As shown in Fig. 3, 2608 and 2610 induced ROS overproduction in a dose-dependent manner on CEM cells. Activation of apoptosis was significant with compound 2608 in COLO 205.

When mitochondria are used to initiate the apoptosis cascade (intrinsic pathway), frequently due to the ROS overproduction, its membrane potential is disrupted during the early stages of the program, ending in its depolarization [71]. Due to mitochondrial depolarization, a downstream effector enzyme, caspase-3, is activated [72]. Caspase-3 is the enzyme where the intrinsic and extrinsic apoptotic pathways converge [73]. Typically, apoptotic cell death is irreversible after caspase-3 is activated [74,75]. To confirm the progression facets of apoptosis induced by the two piperidones, caspase-3/7 activation was evaluated in CEM and COLO 205 cells. As expected, these assays indicated that caspase-3/7 was significantly activated by both piperidines, 2608 and 2610, which agrees with our results. Overall, our findings suggest that both piperidones induce the apoptosis pathway to induce cell death on both cell lines.

The DAPI staining flow cytometry protocol, to measure total cellular DNA contents, was used to examine whether 2608 and 2610 compounds could alter the cell cycle profile and reveal their potential DNA fragmentation activity on CEM and COLO 205 cell lines [39,76–78]. Both 2608 and 2610 did not change the cell cycle profile in the two cell lines tested (Figure 6). More specifically, 2608 induced DNA fragmentation on CEM cells but not in COLO 205 cells. In contrast, 2610 caused DNA fragmentation on both tested cell lines (Figure 6A). Thus, the DNA fragmentation activity of 2608 was selective on CEM cells, whereas 2610 exhibited this activity on both cell lines tested. Also, both 2608 and 2610 compounds did not induce cell cycle arrest. Cells that are undergoing apoptosis display the morphological characteristic of DNA fragmentation[66].

The ubiquitin-proteasome system has been known for the recognition and degradation of misfolded proteins in addition to performing essential roles in DNA replication, cell cycle regulation, cell migration, and immune response [79]. Prior work from our laboratory and others has demonstrated that piperidones induced proteasome inhibition [20]. Piperidone compounds P1 and P2 displayed polyubiquitination and increased Noxa protein expression in HL-60 cells [20]. Due to the similar structure and activity of the compounds, we investigated if the piperidones could also inhibit proteasome activity in both CEM and COLO 205. As demonstrated in previous works, piperidones have been shown to cause the accumulation of polyubiquitinated proteins [22]. Our results revealed that piperidone compound 2610 displayed a strong increase in polyubiquitinated protein accumulation in COLO 205, suggesting the inhibition of the proteome. In comparison, a fold increase was displayed more so in COLO 205 than in CEM for compound 2610. Compound 2608 displayed a moderate increase in polyubiquitinated proteins in both COLO 205 and CEM. In addition, MG 132 displayed slight proteasome inhibition in the CEM cell line in comparison to COLO 205. In light of previous published works with compounds P1 and P2 these data parallel with the polyubiquitination for CEM and COLO 205 once treated with piperidones 2608 and 2610. As been previously shown, the results suggest that these piperidones' cell death induction could be partly due to moderate inhibition of proteasome function [22]. Further work would need to be conducted to advance the understanding of 2608 and 2610 compounds as proteasomal inhibitors. In order to further confirm that said compounds are proteasomal inhibitors, we sought to compare the compounds with piperidone b-AP15, which is a known proteasome inhibitor. Here we characterized compounds 2608

and 2610 that display structural similarity with b-AP15, which have been shown to act as inhibitors of proteasomal associated deubiquitinates (DUBs) [53,80]. Previous work has demonstrated the ability of b-AP15 to inhibit two 19S regulatory DUBs, UCH-L5 and USP-14 [53]. It was also shown that b-AP15 displays cytotoxicity to various cancer cell types, including multiple myeloma cells resistant to the 20S proteasome inhibitor bortezomib, suggesting that proteasome DUB inhibitors may have the clinical potential [56]. Recent studies also support the notion that deubiquitinating enzymes (DUB) are essential factors in proteolytic degradation and that their aberrant activity is linked to cancer progression and chemoresistance [80]. Here we focused primarily on the potential binding affinity of compounds 2608 and 2610 to UCH-L5 and USP-14, seeing as both compounds have a similar structure as b-AP15. With this in mind, the two compounds may also target the same DUBs as b-AP15. Our docking experiments suggested that both piperidones could interact with the same DUBs as b-AP15 and likely inhibit the proteasome similarly to the b-AP15 compound.

In summary, both piperidones were shown to possess favorable cytotoxic properties on 14 cell lines, consisting of hematological cancers and solid tumor cells, from the low nanomolar to the low micromolar range (0.009 μM to 1.664 μM). The two piperidones consistently induced cell death *via* the intrinsic apoptotic pathway, as evidenced and confirmed by the phosphatidylserine (PS) externalization, ROS generation, caspase 3/7 activation, mitochondrial depolarization, and DNA fragmentation for both CEM and COLO 205. Furthermore, the two piperidones exhibited attractive antiproliferative, cytotoxic properties and suitable action mechanisms to be considered potential anticancer drugs.

CHAPTER 3: FURTHER ANALYSIS AND EVALUATION OF F8

3.1 Introduction to thiophene/thiophenecarboxylate compounds

In chapter 3, we continue to screen compounds in our laboratories' chemical library of 30,000 compounds. When a potential cytotoxic compound has been found, we begin to screen the compounds with the same experiments as previously described in order to pinpoint the mechanism of cell death. We will start analyzing the phosphatidylserine externalization, ROS generation, mitochondrial depolarization, cell cycle analysis, and detection of caspase activation.

Thiophene is a five membered heteroaromatic compound containing a sulfur atom at 1 position. It is considered to be a structural alert with formula C_4H_4S, (Figure 10) chemical name is thiacyclopentadiene [81]. Thiophene and its substituent derivatives are very important class of heterocyclic compounds which show interesting applications in the field of medical chemistry [81]. Thiophene like compounds have been reported to possess a wide range of therapeutic properties. Such properties include anti-inflammatory, anti-psychotic, anti-anxiety, kinase inhibiting and anti-cancer [81].

Figure 10 Structure of Thiophene

Microtubules are recognized as crucial components of the mitotic spindle during cell division, and, for this reason, the microtubule system is an attractive target for the development of anticancer agents [82]. With this is mind, thiophene derivatives have

been shown to inhibit tubulin polymerization at the colchicine site [82]. Here we will explore the thiophene derivative and the compounds anti-cancer activity.

A more profitable approach to preventing the proliferation of cancer is multitargeting kinase inhibitors [83]. Previous studies have shown thiophene like compounds inhibiting activity against Pim-1, VEGFR-2, and EGFR [83]. Kinase inhibition of certain biological pathways can potentially aid in halting the over proliferation of cancer cells.

An extensive screening was conducted in order find a potential anti-cancer candidate. Compound F8 (methyl 5-[(dimethylamino)carbonyl]-4-methyl-2-[(3-phenyl-2-propynoyl) amino]-3-thiophenecarboxylate) will be further investigated and tested on various cancer cell lines to display the ability of the compound to induce cell death. This compound is part of a 30,000 compound library that our laboratory is currently analyzing. According to the literature, thiophenecarboxylate like compounds, have been known to act as Epithelial Growth Factor receptor kinase inhibitors, repress cAMP and cGMP in multiple cell lines in response to agonists acting on G-protein-coupled receptors, adenylyl cyclase, and guanylyl cyclase [84,85]. With this in mind, the repression of cAMP is of importance because it regulates cell growth. Studies suggest thiophene derivative compounds displayed high activity with inhibiting Pim-1 kinase [86]. Suggesting, the ability to repress the over proliferation of cells cancer tends to do. Here we present a thiophene derivative.

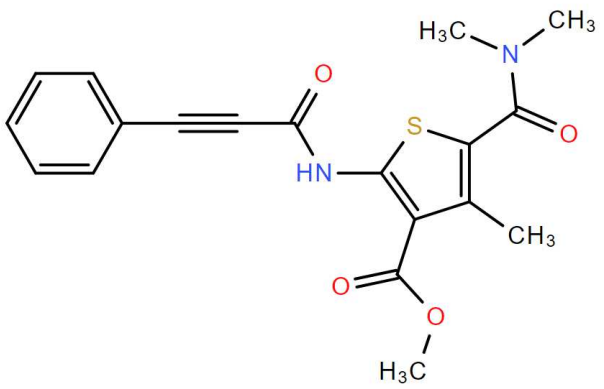

Figure 11: Structure compound of F8, (methyl 5-[(dimethylamino)carbonyl]-4-methyl-2-[(3-phenyl-2-propynoyl)amino]-3-thiophenecarboxylate).

3.2 Evaluate the cytotoxicity of the compound on various cancer cell lines

In order to determine a compounds CC_{50}, Differential Nuclear Staining assays [DNS] will be conducted that uses two DNA intercalators, Hoechst 33342 and Propidium Iodide [PI], that are detected in the flow cytometer and bioimager systems [31]. As previously stated, both of these dyes are able to stain DNA and distinguish between which cells are alive or dead. Hoechst 33342 possesses the ability to stain both live and dead cells, while PI cannot permeate the cell membrane when it is intact and can only stain the nucleic acids (DNA) of cells when its cell membrane is compromised. The treated cells will undergo the same methodology as previously stated with compounds 2608 and 2610. Further evaluation of the cytotoxicity of compound F8 is displayed in Table 3.

Table 3: Compound F8 cytotoxic concentrations (CC_{50}) on various cancer cell lines at a 48 h time point. SCI: selective cytotoxicity index values were calculated using the following equation: CC_{50} of non-cancerous cells divided by the CC_{50} of the cancer cell line. SCI was calculated using the non-cancer cell line.

		F8		
CELL TYPE	**CELL LINE**	**CC_{50} (µM)**	**S.D.**	**SCI***
Acute Lymphoblastic Lymphoma	CEM	0.856	0.356	34.35
Acute Promyelocytic Leukemia	HL-60	1.29	0.356	22.79
Acute T Cell Leukemia	JURKAT	0.805	0.021	36.53
Acute Lymphoblastic Leukemia	NALM-6	1.29	0.155	22.79
Pancreatic Carcinoma	PANC-1	1.48	0.07	19.87
Malignant Melanoma	A373	2.69	0.40	10.93
Breast Adenocarcinoma	MDA-MB-231	3.05	0.32	9.64
Normal Foreskin Epithelial	HS-27	29.41	0.127	-

The data suggests potential selectivity in leukemia and lymphoma cell lines, with the CC_{50} being at or below 1uM. In comparison to the adherent cell lines whose CC_{50} is a above 1 µM.

3.3 Determine the mechanism of action to induce cell death

We sought out to determine the mechanism of death with compound F8 (methyl 5-[(dimethylamino)carbonyl]-4-methyl-2-[(3-phenyl-2-propynoyl) amino]-3-thiophenecarboxylate). We began by conducting a phosphatidylserine externalization assay. As previously stated, this assay measures the externalization of the negatively charged phospholipid. This is done by using the Annexin V protein that couples to the phospholipid due to its charge. Cells were seeded in a 24-well plate at a density of 100,000 cells per well in 1 mL of culture media for CEM cells. Cells were then treated with compound F8 CC_{50} and X2 CC_{50} and incubated for 24 h. Following incubation, the cells were then harvested and washed with ice-cold PBS and centrifuged for 1200 xg for 5 min. The cells were then stained with a mixture of the annexin V-FITC and PI in 100 µl of binding buffer and incubated for 15 minutes on ice. The cells were then resuspended in 400 µl of binding buffer and read immediately in the flow cytometer. For the controls, we used DMSO as a vehicle control, H_20_2 as a positive control, and an untreated control was included as well. Both the controls and the experimentals were assessed in triplicates.

Here we display CEM cells that have been treated with compound F8. Given the data, the same type of trend that was shown in compounds 2608 and 2610 was displayed. Higher apoptotic values were observed with compound F8 as shown in figure 10. We used both CC_{50} and X2 CC_{50} and saw F8 induced a higher percentage of phosphatidylserine externalization than necrosis. Furthermore, with the externalization of phosphatidylserine on the cell surface we sought out to determine what other apoptotic methods the cell undergoes.

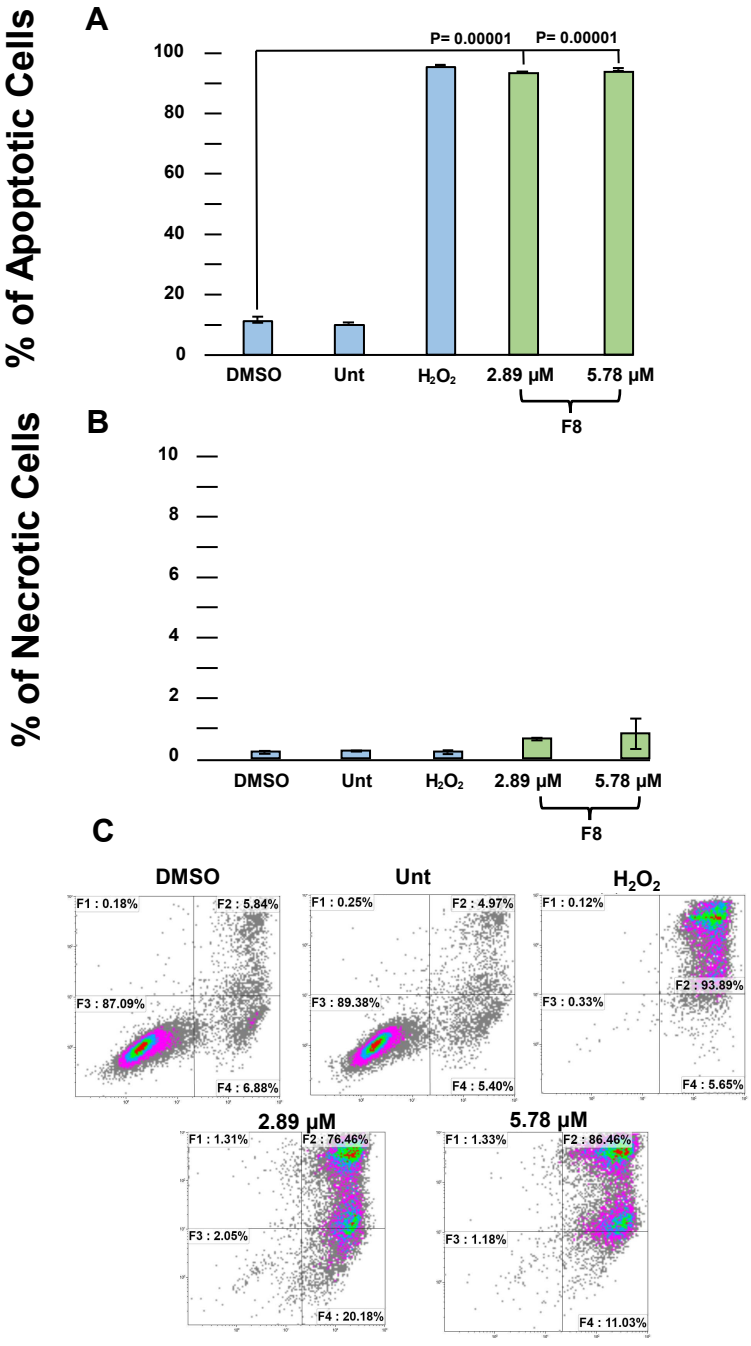

Figure 12: F8 ability to induce apoptosis was assessed in phosphatidylserine externalization assay. Conducted through flow cytometry F8 induced apoptosis in CEM cells. Analysis was performed following a 24 h incubation with 24 h CC_{50} and X2 CC_{50} (2.89

μM and 5.78 μM). Controls included DMSO as the vehicle , H2O2 as the positive, and untreated. Significant phosphatidylserine externalization was evident for the CC_{50} and X2 CC_{50} given the p value p<0.00001 (***).

Assessment of mitochondrial involvement

The accumulation of reactive oxygen species in CEM cells were measured after a treatment of cells after an 18 h incubation. To begin, CEM cells were seeded in a 24-well plate at a density of 100,000 per well in 1 mL of culture medium. CEM cells were treated with F8 CC_{50} and X2 CC_{50} 18 h prior to reading. The same controls that have been used in previous experiments were used in this one as well. Post incubation, cells were collected and placed in flow cytometry tubes and centrifuged for 5 min at 1200 RPM. They were then resuspended in PBS containing carboxy-H2 DCFDA and incubated for 1 h. Cells were then centrifuged and resuspended in 500 μl of PBS. Cells were then analyzed via flow cytometry.

High levels of Reactive Oxygen Species have been known to lead to the depolarization of the mitochondria [44]. With the increase of ROS production, it is known to be responsible for damages in the DNA, proteins, lipids, and may result in the cells overall dysfunction [44]. Here we investigate the mechanism at which F8 induces cell death. Following the exposure, the findings indicate significant depolarization of the mitochondria in comparison to the vehicle control. Thus, the accumulation of ROS was present in CEM cells after the treatment with F8.

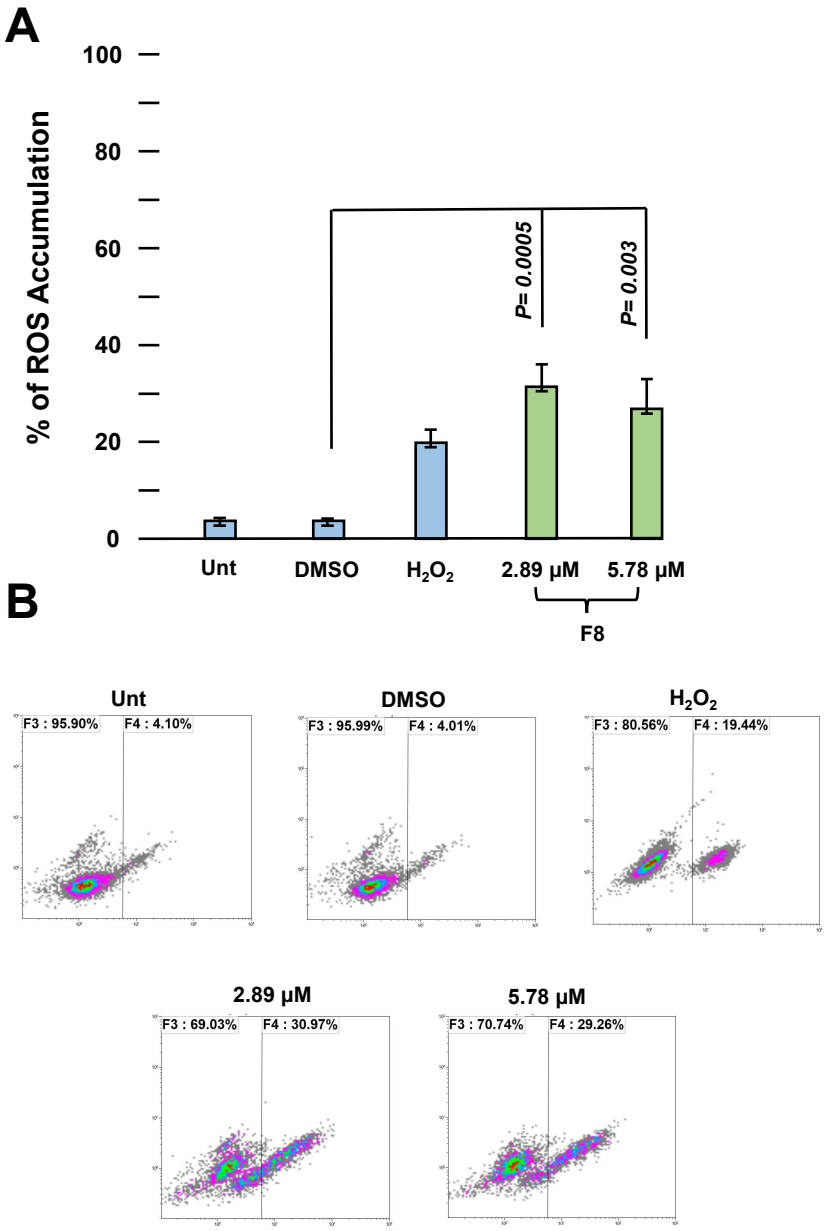

Figure 13: Significant ROS was induced by F8 on CEM cell line in comparison to the vehicle control, DMSO, following an 18 h incubation period. Statistical analyses were acquired using a two-tailed t test, p=0.0005 and p=0.003. Representative dot plots are shown in panel B.

Analysis of mitochondria membrane potential in CEM cells after treatment with F8

CEM cells were seeded in 24- well plates and treated with F8 CC_{50} and X2 CC_{50} for a 4 h incubation. The cells were harvested and labelled with fluorophore 5,5,6,6,-tetraethylbenzimidazolylcarbocyanine iodide (JC-1). The cells were then read in the flow cytometer in order to capture the cells red and green signals. Healthy cells with a polarized mitochondria will emit a red fluorescence signal due to the aggregate formation. A green signal that is given in the flow cytometer indicates a depolarized mitochondrial membrane (JC-1 monomers). The analysis was completed via the flow cytometer. The amount of JC-1 monomers that were detected were twice that of the DMSO control with compound F8.

In regards to the apoptotic pathway there are two processes involved in apoptosis, the extrinsic and the intrinsic. The extrinsic apoptotic pathway is initiated through interaction with the cell surface death receptors, also known as tumor necrosis factor receptors [88]. Death receptors depend on protein-protein interaction, which is critically involved in apoptosis signaling [88]. The intrinsic apoptotic pathway is mediated through intracellular signaling that converge at the mitochondria in response to stress conditions [88]. Internal stimuli such as genetic damage, oxidative stress, hypoxia and other stimuli trigger initiation of the intrinsic mitochondrial pathway [88]. The loss of the mitochondrial membrane potential occurs when the outer membrane is permeabilized as part of the intrinsic apoptotic pathway [89]. We utilized the JC- 1 assay to measure a change in the mitochondrial membrane potential after treatment with thiophene compound F8. In figure 12 we observe a significant number of cells with a depolarized mitochondria, twice that of the control value.

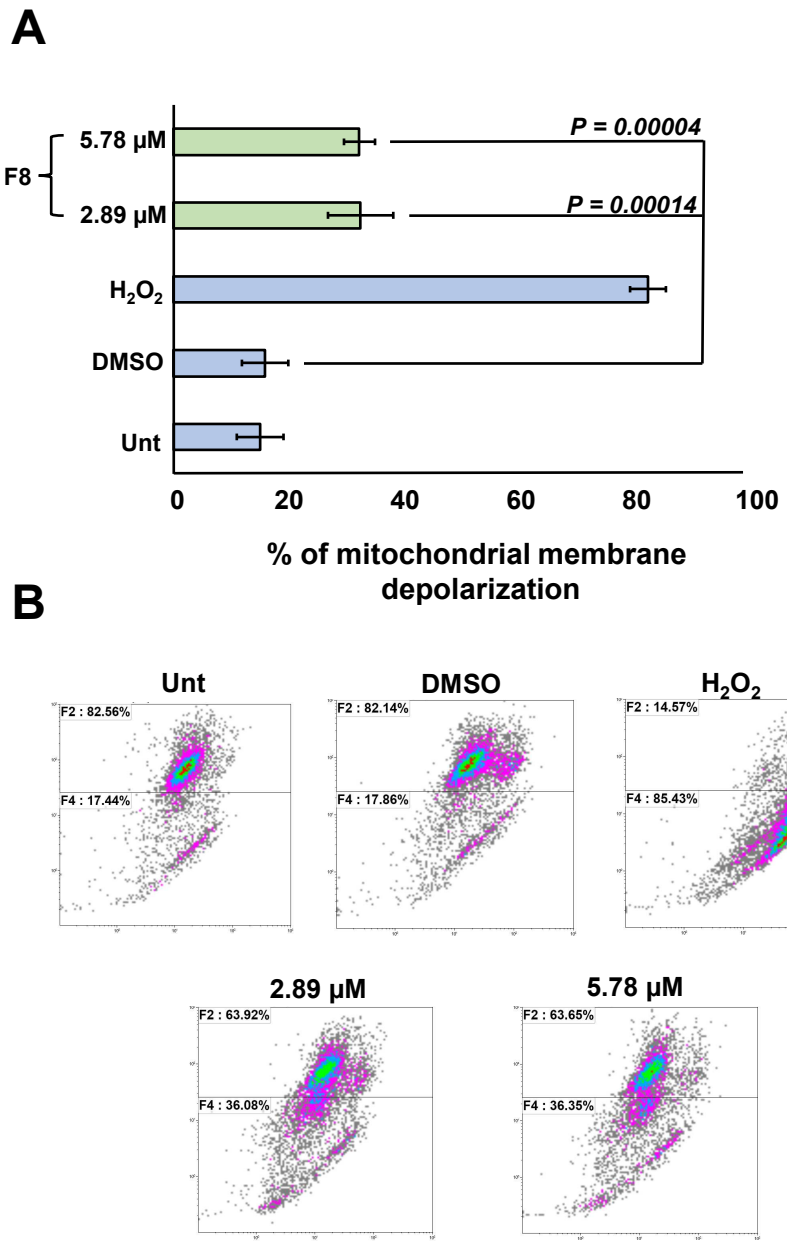

Figure 14: Significant mitochondrial depolarization activity was induced by compound F8 on CEM cells following a 4 h incubation. The cells were stained with JC-1 reagent and analyzed by flow cytometry. Statistical analyses was obtained through the two-tailed Students paired t-test. Controls that were included are the same as previously stated. Representative dot plots are shown in panel B to correspond to CEM cells.

Caspase 3 Activation

We investigated Caspase 3 activation death mechanism to further validate apoptosis. Caspases are essential for the initiation and execution of caspases. Caspases can be divided into 3 groups, initiator caspases (caspase 2, 8, 9, and 10), executioner caspases (caspase 3, 6, and 7) and lastly inflammatory caspases (1, 4, 5, 11, and 12) [90]. Initiator caspases begin the cascade of caspase activation and initiate the apoptotic signal [90]. Upon activation of the executioner caspases, a mass proteolysis occurs, cleaving a range of substrates, including downstream caspases, nucleic proteins, plasma membrane proteins, and mitochondrial membrane proteins, ultimately leading to cell death [90]. Activation of caspase can be detected by certain methods, here we identify the activation of caspase-3 utilizing the fluorogenic NucView 488 caspase-3 substrate. CEM cells were plated at a density of 100,000 cells per well and treated with F8 CC_{50} and X2 CC_{50}. Following the incubation, samples were collected and stained with the fluorogenic NucView 488 according to the manufacturers protocol. Samples were then read immediately via the flow cytometer with 10,000 events per sample. Cells that emitted a green fluorescence were apoptotic cells with an active caspase-3. F8 CC_{50} displayed significant caspase-3 activation in comparison to the vehicle control. In regard to X2 CC_{50}, the same manner of caspase-3 activation was observed in comparison to the vehicle control. Thus, both concentrations for the compounds showed significant caspase-3 activation.

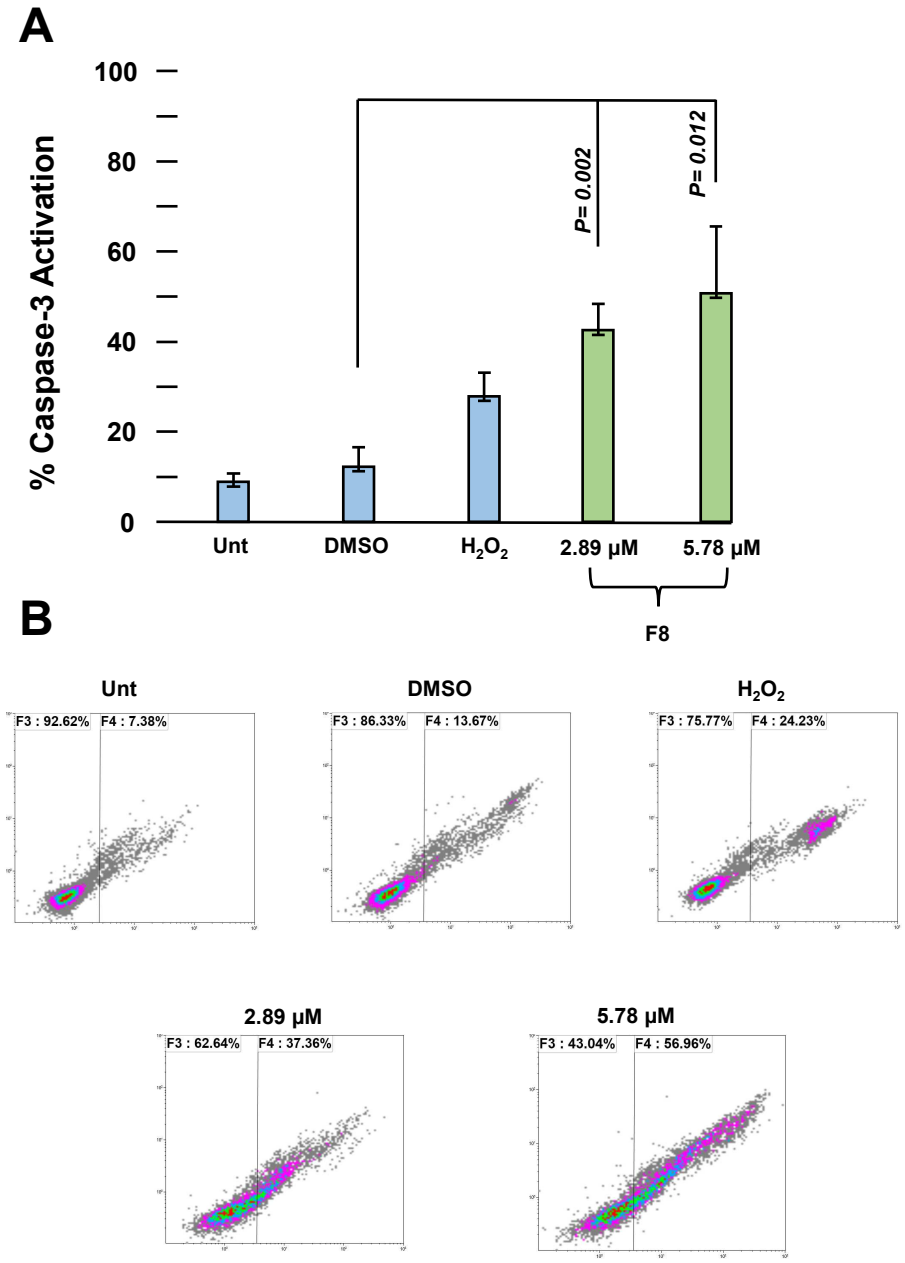

Figure 15: Compound F8 induced significant caspase-3/7 activation in CEM cells. The cells were incubated for a 8 h period and stained with NucView 488 caspase-3/7 substrate. Statistical analyses was obtained using the two-tailed Student's paired t-test in comparison with the vehicle control (1% DMSO). Representative dot plots are shown in panel B to correspond to CEM cells.

Cell Cycle analysis

Our compound F8 has shown characteristics that are conclusive with the apoptotic pathway utilizing the intrinsic pathway. We continue our investigation with analyzing the cell cycle and at which stage the compound causes cell arrest. This assay analyzes different stages of the cell cycle. It is important to note that CC_{50} and lower concentrations were used in order to observe the different stages in the cell cycle. If higher concentrations were to be used, accumulation in the sub G0/G1 phase would be observed. CEM cells were plated at a density of 100,00 cells per well and incubated for a 72 h period with compound F8 CC_{25} and CC_{10}. The same treatments and controls were used in this experiment as presented in other sections. Following the incubation, F8 did not alter the cell cycle in the CEM cell line. As shown, F8 induced DNA fragmentation in CEM cells. Ultimately did not induce cell arrest but did cause DNA fragmentation.

The DAPI protocol was used to measure DNA contents and to examine whether F8 could alter the cell cycle. DAPI is commonly used in cell cycle analyses since it preferentially binds to dsDNA, when the cells have been permeabilized [91]. This allows the DAPI to intercalate and saturate the nucleic acids [91]. The DAPI binds to A-T rich regions of DNA and will fluoresce 20-fold when bound to double stranded DNA [92] This helps quantify the cells in different stages of the cell cycle in the flow cytometer.

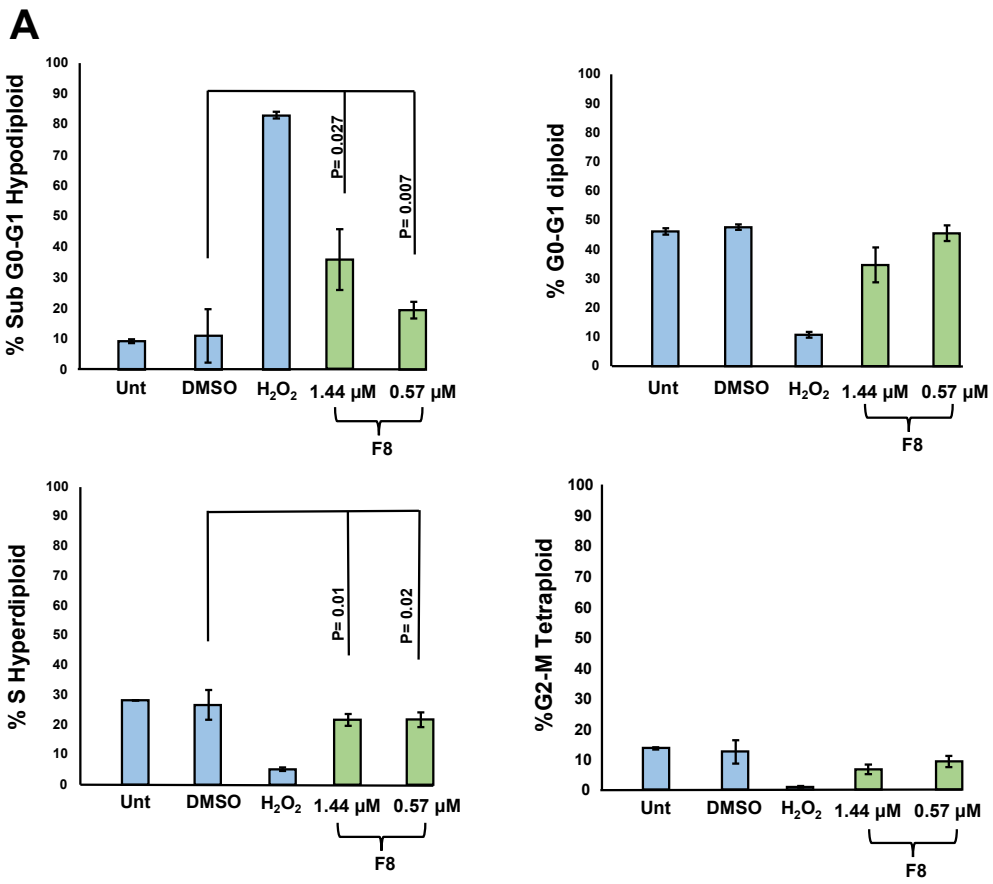
A
% Sub G0-G1 Hypodiploid
P= 0.027
P= 0.007
Unt
DMSO
H2O2
1.44 µM
0.57 µM
F8
% G0-G1 diploid
% S Hyperdiploid
P= 0.01
P= 0.02
%G2-M Tetraploid

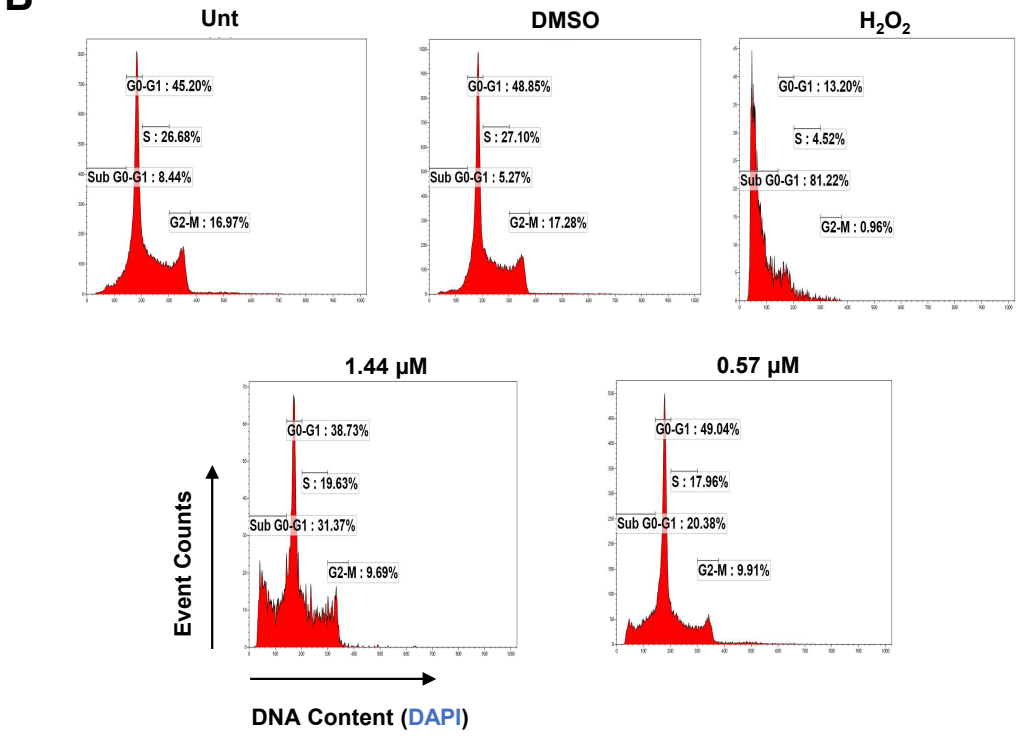
B
Unt
DMSO
H2O2
G0-G1 : 45.20%
S : 26.68%
Sub G0-G1 : 8.44%
G2-M : 16.97%
G0-G1 : 48.85%
S : 27.10%
Sub G0-G1 : 5.27%
G2-M : 17.28%
G0-G1 : 13.20%
S : 4.52%
Sub G0-G1 : 81.22%
G2-M : 0.96%
1.44 µM
0.57 µM
G0-G1 : 38.73%
S : 19.63%
Sub G0-G1 : 31.37%
G2-M : 9.69%
G0-G1 : 49.04%
S : 17.96%
Sub G0-G1 : 20.38%
G2-M : 9.91%
Event Counts
DNA Content (DAPI)

Figure 16: F8 cytotoxicity was analyzed via flow cytometer after a 72 h exposure on CEM cells utilizing 24 h CC_{10} and CC_{25}. NIM-DAPI was used to stain and quantify the amount of DNA in each sample. F8 displays DNA fragmentation evident in the Sub G0-G1 phase. Controls were included, DMSO as the vehicle and H_2O_2 as the positive control, and untreated cells respectively.

3.4 Investigate the inhibition of phosphorylation of F8

The phosphorylation of the MAPK and JAKSTAT were assessed on CEM cells with compound F8 via Human Phosphorylation Pathway Profiling Array C55. Cells were plated at a density of 2.7 x 10^6 per mL and treated with F8 X2 CC_{50}. Following a 3 hour incubation, the cells were harvested and centrifuged. The cells in each sample were then lysed with lysis buffer, a protease inhibitor cocktail, and a phosphatase inhibitor cocktail. The membranes were blocked prior to the samples being added. The sample was then incubated overnight with the MapK and JakStat membranes. The following day the membranes were then washed 5 times with Wash Buffer I (3) and Wash Buffer II (2) for 5 min at RT (room temperature). The detection antibody cocktail was prepared and divided into each well and incubated overnight. The membrane was then washed as previously described. During the washes, 1X HRP-Anti-Rabbit IgG was prepared and divided into each well (1mL) following the washes. The membranes with the added HRP were then incubated overnight. Lastly, the membranes were then washed as directed previously and the membranes were then transferred, printed side up onto a plastic sheet. In a separate tube, 250 µl of detection buffer C and 250 µl of detection buffer D were combined, totaling 500 µl. The detection buffer mixture was placed on each membrane and incubated for 2 minutes at RT (not rocked). Another plastic was placed onto the membrane and a conical tube was rolled gently across to smooth out any air bubbles, making a “sandwich” between two plastics. The sandwiched membranes were then transferred to a chemiluminescence imaging system and exposed.

Following exposure, the data was obtained via densitometry and normalized according to the protocol data analysis. It was observed in the JakStat membrane a reduction in signal in comparison to the DMSO. The fold reduction for Jak1 0.79 in comparison to 1 for DMSO. The fold reduction for Jak and Stat are as follows, Jak 2 0.38, Stat 1 1.02, Stat 2 0.55, Stat 3 0.57, Stat 5 0.32, and Stat 6 4.47. Experimentals that were also included in the membrane include SRC 0.82, TYK 2 0.91, EGFR 1.46, SHP 1 0.54, and SHP 2 0.60. We are going to focus primarily on Jak, Stat and ERK. The effects of Jak Stat signaling and the persistent activation of Stat3 and Stat5 on tumor cell survival, proliferation, and invasion have made the Jak Stat pathway a favorable candidate for cancer therapy [93]. Given the data, there was a reduction on the Jak and Stat pathways suggesting the compound may be inhibiting a very important biological pathway that is responsible for tumor progression. Hyperphosphorylation was also observed in the MapK membrane, with values for ERK 1 5.77 and ERK 2 1.38. MapK associated kinase values in the membrane included CREB 1.62, HSP 27 4.14, JNK 23.72, MEK 7.93, MMK3 1.18, MMK6 3.59, P38 2.08, P53 1.05, RSK 1 1.11, and RSK 2 0.89. Map K are present in the spindle and associated with microtubule organizing centers at the spindle poles and at the cytoplasm [94]. Extracellular signal-regulated kinase (ERK) 1/2 plays crucial roles in cell cycle progression, particularly during M-phase [95] Thus, the hyperphosphorylation of ERK may be contributing to disruption of microtubule formation and preventing cells from entering anaphase [95].

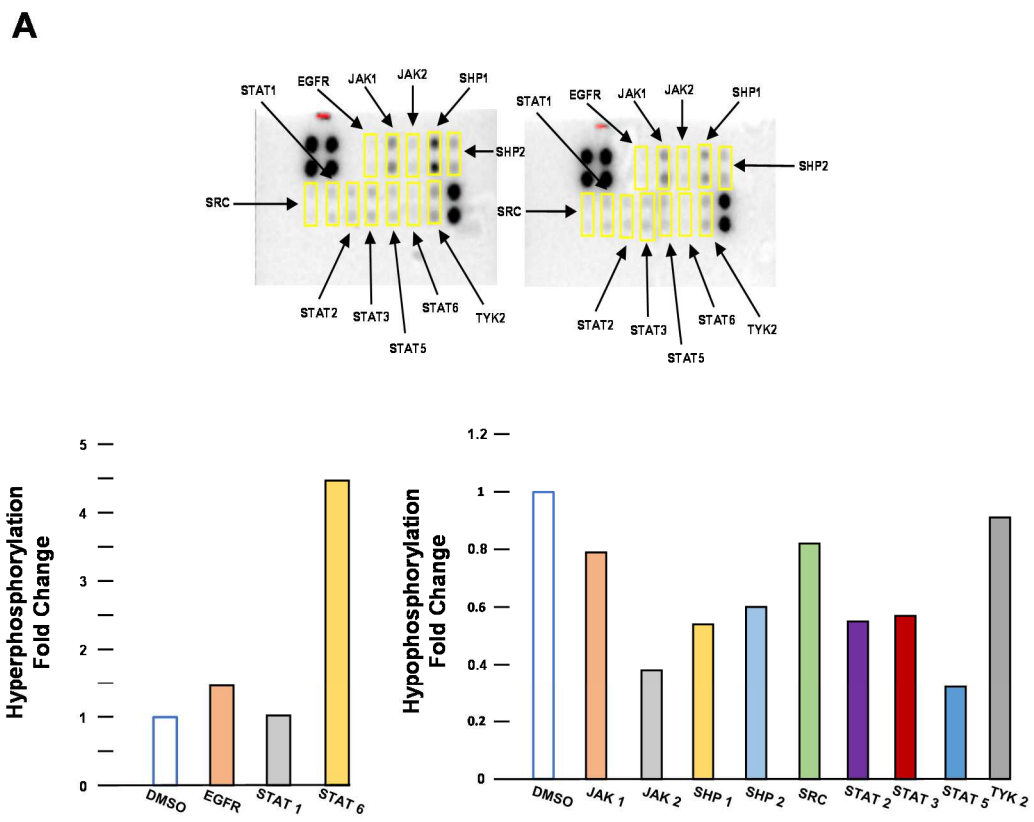
A
STAT1
EGFR
JAK1
JAK2
SHP1
SHP2
SRC
STAT2
STAT3
STAT5
STAT6
TYK2
Hyperphosphorylation Fold Change
DMSO
EGFR
STAT 1
STAT 6
Hypophosphorylation Fold Change
DMSO
JAK 1
JAK 2
SHP 1
SHP 2
SRC
STAT 2
STAT 3
STAT 5
TYK 2
B
CREB
MEK
MKK3
ERK 1/2
JNK
MSK2
HSP27
MMK6
p38
p53
RSK1
RSK2
Hyperphosphorylation Fold Change
DMSO
CREB
ERK 1
ERK 2
HSP27
JNK
MEK
MKK3
MMK6
P38
P53
RSK 1
Hypophosphorylation Fold Change
DMSO
RSK 2

Figure 17:Human Phosphorylation Kinase Array C55 was conducted on the CEM cell line. Utilizing MapK and JakStat membrane in order to gage phosphorylation. Fold changes were determined using densitometry. Hyperphosphorylation was observed in the MapK membrane versus the JakStat. Hypophosphorylation was displayed in the Jak 1-2 and Stat 2-5. It is important to note data displays one experiment.

3.5 Investigation of microtubule inhibition

Microtubule formation was assessed on MDA-MB-231 at a density of 2500 cells per well in a 96 well plate, respectively. Since adherent MDA-MB-231 cells are easily visualized for alterations in their cytoskeleton , they were chosen over the leukemia cell lines. Upon plating the cells were incubated overnight and the cells were treated the following day in triplicates with the experimental compound CC_{50}. The controls that were included were 1 µM final of paclitaxel, this is used as a microtubule disruption control. Cytochalasin-D 5 ug/ml final that acts as an actin polymerization inhibition control and lastly DMSO as the vehicle control. Once treated, the cells were then incubated for 2h. it is important to note the short incubation time is due to wanting to display primary effects of the compound and not secondary. If a longer incubation time would have been conducted, we would be displaying secondary effects of the compound. Following incubation, the cells were fixed by adding 100 µl of fresh 8% formaldehyde without removing any media bringing the final concentration to 4% formaldehyde. Incubate for 20 min at room temp. Remove the formaldehyde from each well, then wash and permeabilize the cells by adding 200 µl of 0.1% Tween 20 detergent in PBS. Incubate for 10 min at room temperature. Repeat the washes two more times without an incubation period. After the washes, remove the Tween PBS solution and add 200 µl of blocking solution, 5% bovine serum albumin in TBS-T (Tris buffer saline with 0.1% Tween 20). Incubated for one hour on a rocking platform at room temperature. Lastly, remove the blocking solution from each well and add 50 µl of PBS solution containing 0.1% Tween 20, DAPI 10 µg/mL, phalloidin

conjugated to Alexa Fluor 568 (0.165 μM) and 0.5 ug/ml tubulin monoclonal antibody conjugated to Alexa Fluor-488. The plate was read via confocal microscopy.

Given the data, in comparison to both positive controls, paclitaxel and cytochalasin-D there was no disruption of actin filaments or microtubule disruption in the experimental F8. Paclitaxel is used to suppress microtubule detachment from centromeres. The role of cytochalasin-D is that it is a permeable fungal toxin that binds to the ends of actin filaments inhibiting the association and disassociation. This data suggests that the compound is not affecting microtubule formation upon early treatment of the cell. The reasoning for a short incubation time is that we needed to observe primary effects of the compound. Longer incubation times would display secondary effects of the compound. Thus, F8 does not disrupt microtubule formation or cytoskeleton organization.

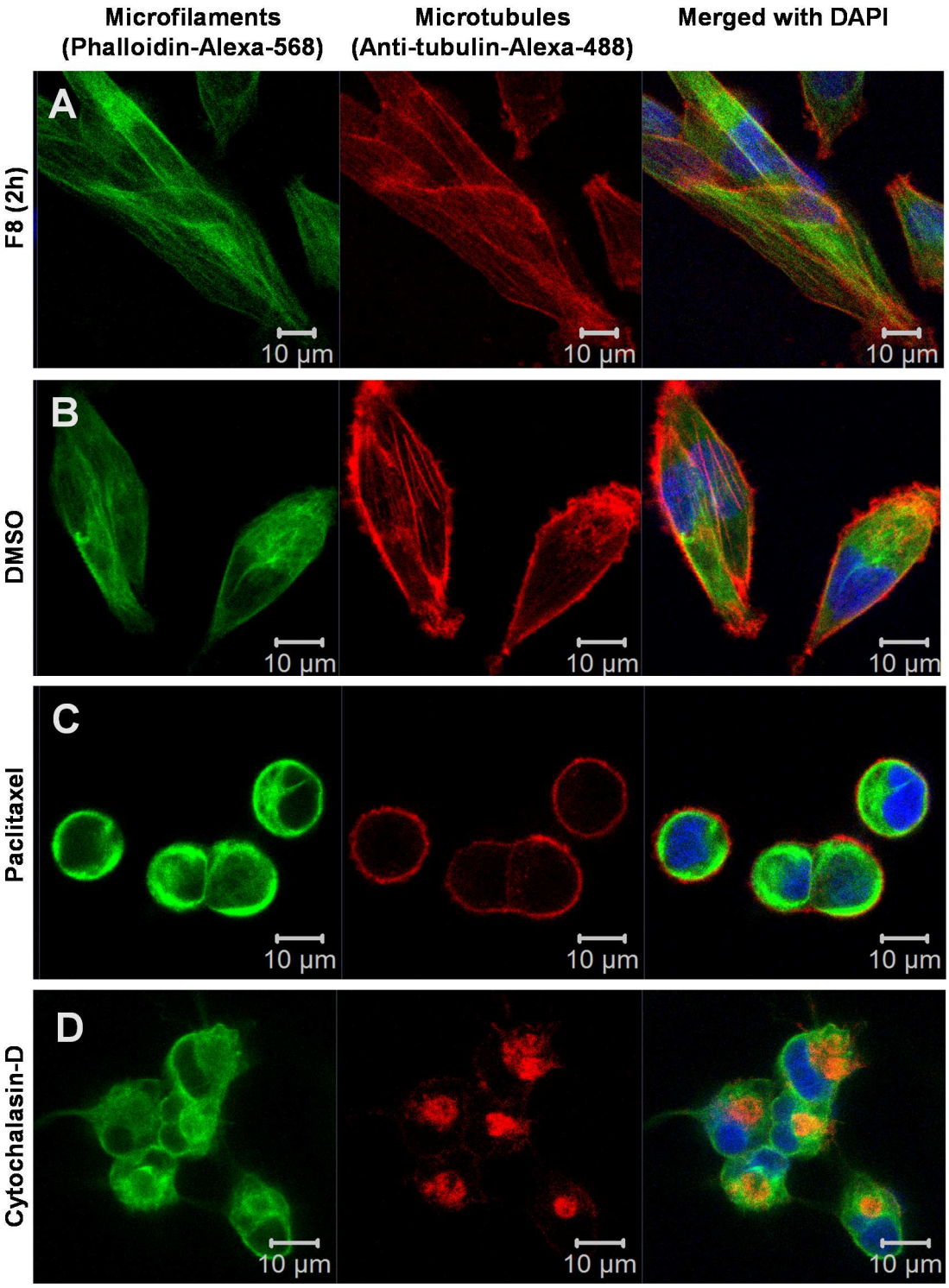

Figure 18: Compound F8 did not disrupt the microfilaments of the cytoskeleton organization in MDA-MB231 cells. The cells were treated for 2h with the compound and triple stained with Alexa-568 conjugated phalloidin, Alexa-488 anti-tubulin, and DAPI. Microscopy images of MDA-MB231 display microfilaments (F-actin; Alexa-568 red channel) and microtubules (tubulin; Alexa-488 green channel) and nucleus (blue channel; DAPI). The left column of images represents microtubules (green), the middle column corresponds to F-actin microfilaments (red), merged images of Alexa-568 and Alexa-488 channels with DAPI channel.

3.6 Discussion

Previously it has been shown that thiophene compounds have the ability to induce apoptosis in cancer cell lines [96]. Thiophenes have been used to treat a variety of cancers and other condition in the U.S. [97]. Thiophenes are a sulfur containing heterocyclic compound that binds with a wide range of cancer specific protein targets, depending on its nature [97]. Here we discuss thiophenecarboxylate compound, F8 and its ability to display cytotoxicity towards cancer cell lines. Here, we explored the compounds cytotoxicity in various cancer cell lines, with CC_{50} values ranging from nanomolar to low micromolar concentrations (0.805 μM to 3.05 μM). Additionally, we demonstrated the compounds' ability to induce apoptosis in the CEM cell line by investigating phosphatidylserine externalization, mitochondrial membrane depolarization, reactive oxygen species generation, and the activation of executioner caspase-3. Following the Annexin V / PI assay, it was concluded that F8 induced cell death via the apoptotic pathway due to the significant PS externalization. With cells undergoing programmed cell death, phosphatidylserine translocate to the outside of the membrane and signals for engulfment [41]. Here we displayed significant phosphatidylserine externalization with compound F8 in CEM cells.

When a cell is undergoing apoptosis, it can go through the intrinsic or extrinsic pathway [67]. The intrinsic pathway releases factors via the mitochondria within the cell [68]. A mitochondrial depolarization assay (JC 1) was conducted to investigate the depolarization of the mitochondria. This tends to occur when the cell is undergoing apoptosis *via* the intrinsic apoptotic pathway. Compound F8 induced significant

depolarization of the mitochondria, thus proving F8 acts via the intrinsic apoptotic pathway.

We studied ROS generation after compound treatment of F8 on CEM cells. The role of ROS is very important, it is released upon the depolarization of the mitochondria's membrane [89]. This overproduction of ROS causes cellular stress, activate caspases, and overall lead to cell death [70]As shown, F8 induced ROS overproduction in CEM cells, thus leading to apoptosis.

By permeabilization of the mitochondrial membrane executioner caspase-3 becomes activated [68]. Typically an apoptotic death is irreversible after caspase-3 is activated [74]. Upon activation, caspases demolish key proteins, cleave DNA and activate other enzymes. Caspase-3 activation was assessed in CEM, following treatment with F8. Significant caspase-3 activation was shown and thus our findings suggest activation of apoptosis via the intrinsic pathway.

A cell cycle analysis was conducted in order to measure cellular DNA content in CEM cells upon treatment of F8. Compound F8 did not change the cell cycle profile in the CEM cell line. More specifically, F8 induced DNA fragmentation. Cells undergoing apoptosis display the morphological characteristic of DNA fragmentation, thus confirming our previous results [66].

A phosphorylation array was conducted on CEM cells with thiophene F8. According to the literature, thiophenes have displayed the ability to inhibit phosphorylation in very important biological pathways [96]. He we sought out to determine if F8 can inhibit phosphorylation in the Map K, Jak, Stat, and ERK pathway. Map Kinase plays an

essential role in extracellular signaling and is often dysregulated in various cancers [98]. Often times, stress-activated pathways, such as Jun N-terminal kinase and p38, largely seem to counteract malignant transformation and here we saw hyperphosphorylation of JNK and p38 [98]. According to the data, hypophosphorylation was observed in Jak 1 and Jak 2. Suggesting inhibition of that pathway upon treatment with compound F8. It was also noticed for Stat 2, Stat 3, and Stat 5 hypophosphorylation was also observed. In regards to ERK 1/2,and CREB it has been shown upon treatment of thiophene derivatives ERK and CREB becomes hypophosphorylated. ERK 1/2 has previously shown to induce apoptosis in human lung carcinoma cells [99]. ERK has also been known to facilitate the transfer of extracellular signals to the nucleus by phosphorylation of certain transcription factors, STAT 3 and CREB. There transcription factors are known proto-oncogenes and are often persistently active in cancer [100–102]. In addition to the hyperphosphorylation in ERK, ERK plays a role in chromosome alignments and microtubule assembly [94,95]. It was theorized that this increase can potentially inhibit microtubule formation. A cytoskeleton analysis was conducted on MDA-MB-231 cell line. According to the data, F8 did not cause disruption in microtubule formation in the cells. Suggesting the compound does not act upon the microtubules and instead acts upon another pathway in the cell. With the phosphorylation data, it can potentially pave the way for future studies in the Jak Stat or MapK pathway.

3.7 Future Work

The research presented in this dissertation are simply small steps towards evaluating 2608, 2610, and F8 as anticancer drugs. Additional studies could include *in-vivo* studies with compounds 2608 and 2610. For compound F8, further analysis of the phosphorylation data could open a realm of possibilities in exploring different pathways the compound takes in the cell. Ultimately, F8 can be evaluated in patients following further exploration.

REFERNECES

1. TL W. The tumor microenvironment and its role in promoting tumor growth. Oncogene [Internet]. Oncogene; 2008 [cited 2021 Jul 13];27:5904–12. Available from: https://pubmed.ncbi.nlm.nih.gov/18836471/

2. Types of Cancer Treatment - National Cancer Institute [Internet]. [cited 2021 Jul 13]. Available from: https://www.cancer.gov/about-cancer/treatment/types

3. Long-Term Side Effects of Cancer Treatment | Cancer.Net [Internet]. [cited 2021 Jul 13]. Available from: https://www.cancer.net/survivorship/long-term-side-effects-cancer-treatment

4. Siegel RL, Miller KD, Fuchs HE, Jemal A. Cancer statistics, 2022. CA Cancer J Clin [Internet]. Wiley; 2022 [cited 2022 Aug 29];72:7–33. Available from: https://www.cancer.org/research/cancer-facts-statistics/all-cancer-facts-figures/cancer-facts-figures-2022.html

5. Pinheiro PS, Callahan KE, Siegel RL, Jin H, Morris CR, Trapido EJ, et al. Cancer Mortality in Hispanic Ethnic Groups. Cancer Epidemiol Biomarkers Prev [Internet]. NIH Public Access; 2017 [cited 2021 Jul 14];26:376. Available from: /pmc/articles/PMC5336466/

6. Report: Cancer Risk Varies Widely Among Hispanic Americans [Internet]. [cited 2021 Jul 14]. Available from: https://www.cancer.org/latest-news/report-cancer-risk-varies-widely-among-hispanic-americans.html

7. RL S, KD M, A GS, SA F, LF B, JC A, et al. Colorectal cancer statistics, 2020. CA Cancer J Clin [Internet]. CA Cancer J Clin; 2020 [cited 2021 Jul 14];70:145–64. Available from: https://pubmed.ncbi.nlm.nih.gov/32133645/

8. Barrington-Trimis JL, Cockburn M, Metayer C, Gauderman WJ, Wiemels J, McKean-Cowdin R. Rising rates of acute lymphoblastic leukemia in Hispanic children: trends in incidence from 1992 to 2011. Blood [Internet]. The American Society of Hematology; 2015 [cited 2021 Jul 14];125:3033. Available from: /pmc/articles/PMC4424421/

9. Yanez B, McGinty HL, Buitrago D, Ramirez AG, Penedo FJ. Cancer Outcomes in Hispanics/Latinos in the United States: An Integrative Review and Conceptual Model of Determinants of Health. J Lat Psychol [Internet]. NIH Public Access; 2016 [cited 2021 Jul 14];4:114. Available from: /pmc/articles/PMC4943845/

10. Risk Factors for Cancer - NCI [Internet]. [cited 2022 Aug 30]. Available from: https://www.cancer.gov/about-cancer/causes-prevention/risk

11. Cooper GM. The Development and Causes of Cancer. Sinauer Associates; 2000 [cited 2022 Aug 30]; Available from: https://www.ncbi.nlm.nih.gov/books/NBK9963/

12. Alhmoud JF, Woolley JF, al Moustafa AE, Malki MI. DNA Damage/Repair Management in Cancers. Cancers (Basel) [Internet]. Multidisciplinary Digital Publishing Institute (MDPI); 2020 [cited 2022 Aug 30];12. Available from: /pmc/articles/PMC7226105/

13. Alhmoud JF, Woolley JF, al Moustafa AE, Malki MI. DNA Damage/Repair Management in Cancers. Cancers (Basel) [Internet]. Cancers (Basel); 2020 [cited 2022 Aug 30];12. Available from: https://pubmed.ncbi.nlm.nih.gov/32340362/

14. Tabas I, Ron D. Integrating the mechanisms of apoptosis induced by endoplasmic reticulum stress. Nat Cell Biol [Internet]. Nat Cell Biol; 2011 [cited 2022 Aug 30];13:184–90. Available from: https://pubmed.ncbi.nlm.nih.gov/21364565/

15. D'Arcy P, Wang X, Linder S. Deubiquitinase inhibition as a cancer therapeutic strategy. Pharmacol Ther. Pergamon; 2015;147:32–54.

16. Targeted Cancer Therapy | Targeted Drug Therapy for Cancer [Internet]. [cited 2022 Aug 31]. Available from: https://www.cancer.org/treatment/treatments-and-side-effects/treatment-types/targeted-therapy/what-is.html

17. McConkey DJ. The integrated stress response and proteotoxicity in cancer therapy. Biochem Biophys Res Commun [Internet]. NIH Public Access; 2017 [cited 2022 Aug 31];482:450. Available from: /pmc/articles/PMC5319732/

18. S J, M D-F, P A. Drug sensitivity in cancer cell lines is not tissue-specific. Mol Cancer [Internet]. Mol Cancer; 2015 [cited 2021 Jul 29];14. Available from: https://pubmed.ncbi.nlm.nih.gov/25881072/

19. Zhou D-Y, Zhang K, Conney AH, Ding N, Cui X-X, Wang H, et al. Synthesis and Evaluation of Curcumin-Related Compounds Containing Benzyl Piperidone for Their Effects on Human Cancer Cells. Chem Pharm Bull (Tokyo). The Pharmaceutical Society of Japan; 2013;61:1149–55.

20. Contreras L, Calderon RI, Varela-Ramirez A, Zhang HY, Quan Y, Das U, et al. Induction of apoptosis via proteasome inhibition in leukemia/lymphoma cells by two potent piperidones. Cellular Oncology [Internet]. Springer Netherlands; 2018 [cited 2021 Jun 13];41:623–36. Available from: https://pubmed.ncbi.nlm.nih.gov/30088262/

21. Hanahan D, Weinberg RA. Hallmarks of cancer: The next generation. Cell [Internet]. Elsevier; 2011 [cited 2022 Aug 31];144:646–74. Available from: http://www.cell.com/article/S0092867411001279/fulltext

22. Contreras L, Medina S, Schiaffino Bustamante AY, Borrego EA, Valenzuela CA, Das U, et al. Three novel piperidones exhibit tumor-selective cytotoxicity on leukemia cells via protein degradation and stress-mediated mechanisms. Pharmacological Reports [Internet]. Springer; 2022 [cited 2022 May 20];74:159. Available from: /pmc/articles/PMC8786778/

23. (US) NI of H, Study BSC. Understanding Cancer. National Institutes of Health (US); 2007 [cited 2021 Jul 20]; Available from: https://www.ncbi.nlm.nih.gov/books/NBK20362/

24. Martin T, Ye L, Sanders A, … JL-MC, 2013 undefined. Cancer invasion and metastasis: molecular and cellular perspective. ncbi.nlm.nih.gov [Internet]. [cited 2021 Jul 20]; Available from: https://www.ncbi.nlm.nih.gov/books/NBK164700/

25. Pfeffer CM, Singh ATK. Apoptosis: A Target for Anticancer Therapy. Int J Mol Sci [Internet]. Multidisciplinary Digital Publishing Institute (MDPI); 2018 [cited 2021 Jul 20];19. Available from: /pmc/articles/PMC5855670/

26. Pavel M, Renna M, Park SJ, Menzies FM, Ricketts T, Füllgrabe J, et al. Contact inhibition controls cell survival and proliferation via YAP/TAZ-autophagy axis. Nature Communications 2018 9:1 [Internet]. Nature Publishing Group; 2018 [cited 2021 Jul 20];9:1–18. Available from: https://www.nature.com/articles/s41467-018-05388-x

27. Das S, da Silva CJ, Silva M de M, Dantas MD de A, de Fátima Â, Góis Ruiz ALT, et al. Highly functionalized piperidines: Free radical scavenging, anticancer activity, DNA interaction and correlation with biological activity. J Adv Res [Internet]. Elsevier B.V.; 2018 [cited 2021 Jun 11];9:51–61. Available from: https://pubmed.ncbi.nlm.nih.gov/30046486/

28. Zhou Y, Gregor VE, Ayida BK, Winters GC, Sun Z, Murphy D, et al. Synthesis and SAR of 3,5-diamino-piperidine derivatives: Novel antibacterial translation inhibitors as aminoglycoside mimetics. Bioorg Med Chem Lett [Internet]. Bioorg Med Chem Lett; 2007 [cited 2021 Jun 11];17:1206–10. Available from: https://pubmed.ncbi.nlm.nih.gov/17188860/

29. Misra M, Pandey SK, Pandey VP, Pandey J, Tripathi R, Tripathi RP. Organocatalyzed highly atom economic one pot synthesis of tetrahydropyridines as antimalarials. Bioorg Med Chem. Pergamon; 2009;17:625–33.

30. Rao KN, Redda KK, Onayemi FY, Melles H, Choi J. Synthesis of some N-[pyridyl(phenyl)carbonylamino]hydroxyalkyl-(benzyl)-1,2,3,6-tetrahydropyridines as potential anti-inflammatory agents. J Heterocycl Chem [Internet]. John Wiley & Sons, Ltd; 1995 [cited 2021 Jun 11];32:307–15. Available from: https://onlinelibrary.wiley.com/doi/full/10.1002/jhet.5570320151

31. Aeluri R, Alla M, Bommena VR, Murthy R, Jain N. Synthesis and antiproliferative activity of polysubstituted tetrahydropyridine and piperidin-4-one-3-carboxylate derivatives. Asian J Org Chem [Internet]. Wiley-VCH Verlag; 2012 [cited 2021 Jun 11];1:71–9. Available from: https://onlinelibrary.wiley.com/doi/full/10.1002/ajoc.201200010

32. L C, RI C, A V-R, HY Z, Y Q, U D, et al. Induction of apoptosis via proteasome inhibition in leukemia/lymphoma cells by two potent piperidones. Cell Oncol (Dordr)

[Internet]. Cell Oncol (Dordr); 2018 [cited 2021 Jul 21];41:623–36. Available from: https://pubmed.ncbi.nlm.nih.gov/30088262/

33. Swain RM, Contreras L, Varela-Ramirez A, Hossain M, Das U, Valenzuela CA, et al. Two novel piperidones induce apoptosis and antiproliferative effects on human prostate and lymphoma cancer cell lines. Investigational New Drugs 2022 40:5 [Internet]. Springer; 2022 [cited 2022 Aug 24];40:905–21. Available from: https://link.springer.com/article/10.1007/s10637-022-01266-y

34. Zhang SL, Hu X, Zhang W, Yao H, Tam KY. Development of pyruvate dehydrogenase kinase inhibitors in medicinal chemistry with particular emphasis as anticancer agents [Internet]. Drug Discov Today. Elsevier Ltd; 2015 [cited 2021 Jun 14]. p. 1112–9. Available from: https://pubmed.ncbi.nlm.nih.gov/25842042/

35. Das S, Gul HI, Das U, Balzarini J, Dimmock SG, Dimmock JR. Novel Conjugated Unsaturated Ketones with Submicromolar Potencies Towards some Leukemic and Colon Cancer Cells. Med Chem (Los Angeles) [Internet]. Bentham Science Publishers Ltd.; 2018 [cited 2021 Jun 14];15:430–8. Available from: https://pubmed.ncbi.nlm.nih.gov/30324886/

36. Hossain M, Das U, Dimmock JR. Recent advances in α,β-unsaturated carbonyl compounds as mitochondrial toxins [Internet]. Eur J Med Chem. Elsevier Masson SAS; 2019 [cited 2021 Jun 14]. Available from: https://pubmed.ncbi.nlm.nih.gov/31539776/

37. Das U, Alcorn J, Shrivastav A, Sharma RK, de Clercq E, Balzarini J, et al. Design, synthesis and cytotoxic properties of novel 1-[4-(2-alkylaminoethoxy)phenylcarbonyl]-3,5-bis(arylidene)-4-piperidones and related compounds. Eur J Med Chem. Elsevier Masson; 2007;42:71–80.

38. Lema C, Varela-Ramirez A, Aguilera RJ. Differential nuclear staining assay for high-throughput screening to identify cytotoxic compounds. Curr Cell Biochem [Internet]. NIH Public Access; 2011 [cited 2021 Jul 20];1(1):1–14. Available from: /pmc/articles/PMC4816492/

39. Robles-Escajeda E, Das U, Ortega NM, Parra K, Francia G, Dimmock JR, et al. A novel curcumin-like dienone induces apoptosis in triple-negative breast cancer cells. Cellular Oncology [Internet]. Springer Netherlands; 2016 [cited 2021 Jun 13];39:265–77. Available from: https://pubmed.ncbi.nlm.nih.gov/26920032/

40. HenrÍquez G, Mendez L, Varela-Ramirez A, Guerrero E, Narayan M. Neuroprotective Effect of Brazilin on Amyloid β (25-35)-Induced Pathology in a Human Neuroblastoma Model. ACS Omega [Internet]. American Chemical Society; 2020 [cited 2021 Jun 13];5:13785–92. Available from: https://pubmed.ncbi.nlm.nih.gov/32566844/

41. Robles-Escajeda E, Lerma D, Nyakeriga AM, Ross JA, Kirken RA, Aguilera RJ, et al. Searching in Mother Nature for Anti-Cancer Activity: Anti-Proliferative and Pro-Apoptotic Effect Elicited by Green Barley on Leukemia/Lymphoma Cells. PLoS One

[Internet]. Public Library of Science; 2013 [cited 2021 Jun 11];8:73508. Available from: /pmc/articles/PMC3767772/

42. Robles-Escajeda E, Martínez A, Varela-Ramirez A, Sánchez-Delgado RA, Aguilera RJ. Analysis of the cytotoxic effects of ruthenium-ketoconazole and ruthenium-clotrimazole complexes on cancer cells. Cell Biol Toxicol [Internet]. Kluwer Academic Publishers; 2013 [cited 2021 Jun 13];29:431–43. Available from: /pmc/articles/PMC4207122/

43. Santiago-Vázquez Y, Das U, Varela-Ramirez A, T. Baca S, Ayala-Marin Y, Lema C, et al. Tumor-selective Cytotoxicity of a Novel Pentadiene Analogue on Human Leukemia/lymphoma Cells. Clin Cancer Drugs [Internet]. Bentham Science Publishers Ltd.; 2016 [cited 2021 Jun 13];3:138–46. Available from: /pmc/articles/PMC5110259/

44. Suski JM, Lebiedzinska M, Bonora M, Pinton P, Duszynski J, Wieckowski MR. Relation between mitochondrial membrane potential and ROS formation. Methods in Molecular Biology [Internet]. Methods Mol Biol; 2012 [cited 2021 Jun 11];810:183–205. Available from: https://pubmed.ncbi.nlm.nih.gov/22057568/

45. Torres-Roca JF, Lecoeur H, Amatore C, Gougeon ML. The early intracellular production of a reactive oxygen intermediate mediates apoptosis in dexamethasone-treated thymocytes. Cell Death Differ [Internet]. 1995 [cited 2021 Jun 11];2(4):309–19. Available from: https://pubmed.ncbi.nlm.nih.gov/17180036/

46. Gutierrez DA, DeJesus RE, Contreras L, Rodriguez-Palomares IA, Villanueva PJ, Balderrama KS, et al. A new pyridazinone exhibits potent cytotoxicity on human cancer cells via apoptosis and poly-ubiquitinated protein accumulation. Cell Biol Toxicol [Internet]. Springer; 2019 [cited 2021 Jun 13];35:503–19. Available from: https://europepmc.org/articles/PMC6800828

47. Redza-Dutordoir M, Averill-Bates DA. Activation of apoptosis signalling pathways by reactive oxygen species. Biochimica et Biophysica Acta (BBA) - Molecular Cell Research. Elsevier; 2016;1863:2977–92.

48. Morán-Santibañez K, Vasquez AH, Varela-Ramirez A, Henderson V, Sweeney J, Odero-Marah V, et al. Larrea tridentata extract mitigates oxidative stress-induced cytotoxicity in human neuroblastoma SH-SY5Y cells. Antioxidants [Internet]. MDPI AG; 2019 [cited 2021 Jun 17];8. Available from: https://pubmed.ncbi.nlm.nih.gov/31557847/

49. Degterev A, Boyce M, Yuan J. A decade of caspases [Internet]. Oncogene. Oncogene; 2003 [cited 2021 Jun 11]. p. 8543–67. Available from: https://pubmed.ncbi.nlm.nih.gov/14634618/

50. Donoso-Bustamante V, Borrego EA, Schiaffino-Bustamante Y, Gutiérrez DA, Millas-Vargas JP, Fuentes-Retamal S, et al. An acylhydroquinone derivative produces OXPHOS uncoupling and sensitization to BH3 mimetic ABT-199 (Venetoclax) in human

promyelocytic leukemia cells. Bioorg Chem [Internet]. Academic Press Inc.; 2020 [cited 2021 Jun 17];100. Available from: https://pubmed.ncbi.nlm.nih.gov/32454391/

51. Villanueva PJ, Martinez A, Baca ST, DeJesus RE, Larragoity M, Contreras L, et al. Pyronaridine exerts potent cytotoxicity on human breast and hematological cancer cells through induction of apoptosis. PLoS One [Internet]. Public Library of Science; 2018 [cited 2021 Jun 13];13. Available from: https://pubmed.ncbi.nlm.nih.gov/30395606/

52. ECL (Enhanced Chemiluminescence) Reagents: Enhanced How? [Internet]. [cited 2021 Jun 14]. Available from: https://info.gbiosciences.com/blog/ecl-enhanced-chemiluminescence-reagents-enhanced-how

53. D'Arcy P, Brnjic S, Olofsson MH, Fryknäs M, Lindsten K, de Cesare M, et al. Inhibition of proteasome deubiquitinating activity as a new cancer therapy. Nat Med [Internet]. Nat Med; 2011 [cited 2021 Jun 14];17:1636–40. Available from: https://pubmed.ncbi.nlm.nih.gov/22057347/

54. Mujtaba T, Dou QP. Advances in the Understanding of Mechanisms and Therapeutic Use of Bortezomib. Discov Med [Internet]. NIH Public Access; 2011 [cited 2022 Mar 28];12:471–80. Available from: /pmc/articles/PMC4139918/

55. TI D, NS A, OI O, DS M, OE E, GO E, et al. Molecular docking analysis of phyto-constituents from Cannabis sativa with pfDHFR. Bioinformation [Internet]. Bioinformation; 2018 [cited 2021 Sep 5];14:574–9. Available from: https://pubmed.ncbi.nlm.nih.gov/31223216/

56. Wang X, D'Arcy P, Caulfield TR, Paulus A, Chitta K, Mohanty C, et al. Synthesis and Evaluation of Derivatives of the Proteasome Deubiquitinase Inhibitor b-AP15. Chem Biol Drug Des [Internet]. NIH Public Access; 2015 [cited 2021 Sep 5];86:1036. Available from: /pmc/articles/PMC4846425/

57. Lam YA, Xu W, DeMartino GN, Cohen RE. Editing of ubiquitin conjugates by an isopeptidase in the 26S proteasome. Nature 1997 385:6618 [Internet]. Nature Publishing Group; 1997 [cited 2021 Sep 14];385:737–40. Available from: https://www.nature.com/articles/385737a0

58. Yao T, Cohen RE. A cryptic protease couples deubiquitination and degradation by the proteasome. Nature 2002 419:6905 [Internet]. Nature Publishing Group; 2002 [cited 2021 Sep 14];419:403–7. Available from: https://www.nature.com/articles/nature01071

59. Leggett DS, Hanna J, Borodovsky A, Crosas B, Schmidt M, Baker RT, et al. Multiple Associated Proteins Regulate Proteasome Structure and Function. Mol Cell [Internet]. Elsevier; 2002 [cited 2021 Sep 14];10:495–507. Available from: http://www.cell.com/article/S109727650200638X/fulltext

60. Borodovsky A, Kessler BM, Casagrande R, Overkleeft HS, Wilkinson KD, Ploegh HL. A novel active site-directed probe specific for deubiquitylating enzymes reveals proteasome association of USP14. EMBO J [Internet]. European Molecular Biology

Organization; 2001 [cited 2021 Sep 14];20:5187. Available from: /pmc/articles/PMC125629/

61. Kish-Trier E, Hill CP. Structural Biology of the Proteasome. Annu Rev Biophys [Internet]. NIH Public Access; 2013 [cited 2021 Sep 14];42:29. Available from: /pmc/articles/PMC4878838/

62. Tomko RJ, Jr., Hochstrasser M. Molecular Architecture and Assembly of the Eukaryotic Proteasome. Annu Rev Biochem [Internet]. NIH Public Access; 2013 [cited 2021 Sep 14];82:415–45. Available from: /pmc/articles/PMC3827779/

63. Chadchankar J, Korboukh V, Conway LC, Wobst HJ, Walker CA, Doig P, et al. Inactive USP14 and inactive UCHL5 cause accumulation of distinct ubiquitinated proteins in mammalian cells. PLoS One [Internet]. Public Library of Science; 2019 [cited 2021 Sep 14];14. Available from: /pmc/articles/PMC6839854/

64. Das U, Alcorn J, Shrivastav A, Sharma RK, de Clercq E, Balzarini J, et al. Design, synthesis and cytotoxic properties of novel 1-[4-(2-alkylaminoethoxy)phenylcarbonyl]-3,5-bis(arylidene)-4-piperidones and related compounds. Eur J Med Chem. Elsevier Masson; 2007;42:71–80.

65. Varela-Ramirez A, Costanzo M, Carrasco YP, Pannell KH, Aguilera RJ. Cytotoxic effects of two organotin compounds and their mode of inflicting cell death on four mammalian cancer cells. Cell Biol Toxicol [Internet]. Cell Biol Toxicol; 2011 [cited 2021 Jun 13];27:159–68. Available from: https://pubmed.ncbi.nlm.nih.gov/21069563/

66. Alberts B, Johnson A, Lewis J, Raff M, Roberts K, Walter P. Molecular Biology of the Cell. Programmed Cell Death (Apoptosis) [Internet]. Garland Science; 2002 [cited 2021 Jun 13]. Available from: https://www.ncbi.nlm.nih.gov/books/NBK26873/

67. Carneiro BA, El-Deiry WS. Targeting apoptosis in cancer therapy. Nat Rev Clin Oncol [Internet]. NIH Public Access; 2020 [cited 2022 Mar 29];17:395. Available from: /pmc/articles/PMC8211386/

68. Fulda S, Debatin KM. Extrinsic versus intrinsic apoptosis pathways in anticancer chemotherapy [Internet]. Oncogene. Oncogene; 2006 [cited 2021 Jun 13]. p. 4798–811. Available from: https://pubmed.ncbi.nlm.nih.gov/16892092/

69. Kroemer G, Galluzzi L, Brenner C. Mitochondrial membrane permeabilization in cell death. Physiol Rev [Internet]. American Physiological Society; 2007 [cited 2022 May 16];87:99–163. Available from: https://journals.physiology.org/doi/full/10.1152/physrev.00013.2006

70. Wu CC, Bratton SB. Regulation of the intrinsic apoptosis pathway by reactive oxygen species [Internet]. Antioxid Redox Signal. Antioxid Redox Signal; 2013 [cited 2021 Jun 13]. p. 546–58. Available from: https://pubmed.ncbi.nlm.nih.gov/22978471/

71. Loeffler M, Kroemer G. The mitochondrion in cell death control: Certainties and incognita. Exp Cell Res [Internet]. Academic Press Inc.; 2000 [cited 2021 Jun 14];256:19–26. Available from: https://pubmed.ncbi.nlm.nih.gov/10739647/

72. Henderson CJ, Aleo E, Fontanini A, Maestro R, Paroni G, Brancolini C. Caspase activation and apoptosis in response to proteasome inhibitors. Cell Death Differ [Internet]. Nature Publishing Group; 2005 [cited 2021 Jun 14];12:1240–54. Available from: www.nature.com/cdd

73. Li H, Zhu H, Xu CJ, Yuan J. Cleavage of BID by caspase 8 mediates the mitochondrial damage in the Fas pathway of apoptosis. Cell [Internet]. Cell Press; 1998 [cited 2021 Jun 14];94:491–501. Available from: https://pubmed.ncbi.nlm.nih.gov/9727492/

74. Lund T, Stokke T, Olsen E, Fodstad. Garlic arrests MDA-MB-435 cancer cells in mitosis, phosphorylates the proapoptotic BH3-only protein BimEL and induces apoptosis. Br J Cancer [Internet]. Br J Cancer; 2005 [cited 2021 Jun 14];92:1773–81. Available from: https://pubmed.ncbi.nlm.nih.gov/15827557/

75. Ferguson PJ, Kurowska E, Freeman DJ, Chambers AF, Koropatnick DJ. A flavonoid fraction from cranberry extract inhibits proliferation of human tumor cell lines. J Nutr [Internet]. J Nutr; 2004 [cited 2022 Mar 29];134:1529–35. Available from: https://pubmed.ncbi.nlm.nih.gov/15173424/

76. Nakamura-Bencomo S, Gutierrez DA, Robles-Escajeda E, Iglesias-Figueroa B, Siqueiros-Cendón TS, Espinoza-Sánchez EA, et al. Recombinant human lactoferrin carrying humanized glycosylation exhibits antileukemia selective cytotoxicity, microfilament disruption, cell cycle arrest, and apoptosis activities. Invest New Drugs [Internet]. Springer; 2021 [cited 2022 Feb 27];39:400–15. Available from: https://link.springer.com/article/10.1007/s10637-020-01020-2

77. Gutierrez DA, Contreras L, Villanueva PJ, Borrego EA, Morán-Santibañez K, Hess JD, et al. Identification of a Potent Cytotoxic Pyrazole with Anti-Breast Cancer Activity That Alters Multiple Pathways. Cells [Internet]. MDPI; 2022 [cited 2022 Feb 27];11:254. Available from: https://www.mdpi.com/2073-4409/11/2/254/htm

78. Donoso-Bustamante V, Borrego EA, Schiaffino-Bustamante Y, Gutiérrez DA, Millas-Vargas JP, Fuentes-Retamal S, et al. An acylhydroquinone derivative produces OXPHOS uncoupling and sensitization to BH3 mimetic ABT-199 (Venetoclax) in human promyelocytic leukemia cells. Bioorg Chem. Academic Press; 2020;100:103935.

79. Melvin AT, Woss GS, Park JH, Waters ML, Allbritton NL. Measuring Activity in the Ubiquitin-Proteasome System: From Large Scale Discoveries to Single Cells Analysis. Cell Biochem Biophys [Internet]. Springer; 2013 [cited 2021 Jun 14];67:75–89. Available from: https://link.springer.com/article/10.1007/s12013-013-9621-9

80. Coughlin K, Anchoori R, Iizuka Y, Meints J, MacNeill L, Vogel RI, et al. Small-Molecule RA-9 Inhibits Proteasome-Associated DUBs and Ovarian Cancer In Vitro and In Vivo via Exacerbating Unfolded Protein Responses. Clinical Cancer Research [Internet]. American Association for Cancer Research; 2014 [cited 2021 Sep 5];20:3174–86. Available from: https://clincancerres.aacrjournals.org/content/20/12/3174

81. Shah R, Verma PK. Therapeutic importance of synthetic thiophene. Chem Cent J [Internet]. BioMed Central Ltd.; 2018 [cited 2022 Aug 29];12:1–22. Available from: https://bmcchem.biomedcentral.com/articles/10.1186/s13065-018-0511-5

82. Romagnoli R, Kimatrai Salvador M, Schiaffino Ortega S, Baraldi PG, Oliva P, Baraldi S, et al. 2-Alkoxycarbonyl-3-arylamino-5-substituted thiophenes as a novel class of antimicrotubule agents: Design, synthesis, cell growth and tubulin polymerization inhibition. Eur J Med Chem [Internet]. NIH Public Access; 2018 [cited 2022 Aug 30];143:683. Available from: /pmc/articles/PMC5791907/

83. Alamshany ZM, Tashkandi NY, Othman IMM, Anwar MM, Nossier ES. New thiophene, thienopyridine and thiazoline-based derivatives: Design, synthesis and biological evaluation as antiproliferative agents and multitargeting kinase inhibitors. Bioorg Chem [Internet]. Bioorg Chem; 2022 [cited 2022 Sep 1];127:105964. Available from: https://pubmed.ncbi.nlm.nih.gov/35759881/

84. Li S, Sun X, Zhao H, Tang Y, Lan M. Discovery of novel EGFR tyrosine kinase inhibitors by structure-based virtual screening. Bioorg Med Chem Lett. Pergamon; 2012;22:4004–9.

85. Tradtrantip L, Yangthara B, Padmawar P, Morrison C, Verkman AS. Thiophenecarboxylate Suppressor of Cyclic Nucleotides Discovered in a Small-Molecule Screen Blocks Toxin-Induced Intestinal Fluid Secretion. Mol Pharmacol [Internet]. American Society for Pharmacology and Experimental Therapeutics; 2009 [cited 2022 Aug 24];75:134. Available from: /pmc/articles/PMC2685055/

86. Mohareb RM, Wardakhan WW, Abbas NS. Synthesis of Tetrahydrobenzo[b]thiophene-3-carbohydrazide Derivatives as Potential Anti-cancer Agents and Pim-1 Kinase Inhibitors. Anticancer Agents Med Chem [Internet]. Anticancer Agents Med Chem; 2019 [cited 2022 Aug 30];19:1737–53. Available from: https://pubmed.ncbi.nlm.nih.gov/30947678/

87. Differential nuclear staining assay for high-throughput screening to identify cytotoxic compounds - PubMed [Internet]. [cited 2021 Jun 13]. Available from: https://pubmed.ncbi.nlm.nih.gov/27042697/

88. Pistritto G, Trisciuoglio D, Ceci C, Alessia Garufi, D'Orazi G. Apoptosis as anticancer mechanism: function and dysfunction of its modulators and targeted therapeutic strategies. Aging (Albany NY) [Internet]. Impact Journals, LLC; 2016 [cited 2022 Sep 4];8:603. Available from: /pmc/articles/PMC4925817/

89. Tait SWG, Green DR. Mitochondria and cell death: outer membrane permeabilization and beyond. Nat Rev Mol Cell Biol [Internet]. Nat Rev Mol Cell Biol; 2010 [cited 2022 Sep 4];11:621–32. Available from: https://pubmed.ncbi.nlm.nih.gov/20683470/

90. Role of caspases in apoptosis | Abcam [Internet]. [cited 2022 Sep 5]. Available from: https://www.abcam.com/kits/role-of-caspases-in-apoptosis

91. Cell Cycle Determination Using DAPI-Alcohol Fixation Method. [cited 2022 Sep 8]; Available from: https://catalog.invitrogen.com/index.cfm?fuseaction=viewCatalog.viewProductDetails&productDescription

92. DAPI Stain Supplier | CAS 28718-90-3 | Tocris Bioscience [Internet]. [cited 2022 Sep 8]. Available from: https://www.tocris.com/products/dapi_5748?msclkid=353cfae47669157f838e99ff98abda58&utm_source=bing&utm_medium=cpc&utm_campaign=Product%20Type-Fluorescent%20Probes_Top%20Small%20Molecule&utm_term=dapi&utm_content=DAPI_Small%20Molecule_5748

93. Groner B, von Manstein V. Jak Stat signaling and cancer: Opportunities, benefits and side effects of targeted inhibition. Mol Cell Endocrinol [Internet]. Mol Cell Endocrinol; 2017 [cited 2022 Sep 22];451:1–14. Available from: https://pubmed.ncbi.nlm.nih.gov/28576744/

94. Verlhac MH, de Pennart H, Maro B, Cobb MH, Clarke HJ. MAP Kinase Becomes Stably Activated at Metaphase and Is Associated with Microtubule-Organizing Centers during Meiotic Maturation of Mouse Oocytes. Dev Biol. Academic Press; 1993;158:330–40.

95. Iwamoto E, Ueta N, Matsui Y, Kamijo K, Kuga T, Saito Y, et al. ERK Plays a Role in Chromosome Alignment and Participates in M-Phase Progression. J Cell Biochem [Internet]. John Wiley & Sons, Ltd; 2016 [cited 2022 Sep 22];117:1340–51. Available from: https://onlinelibrary.wiley.com/doi/full/10.1002/jcb.25424

96. Hess JD, Macias LH, Gutierrez DA, Moran-Santibanez K, Contreras L, Medina S, et al. Identification of a Unique Cytotoxic Thieno[2,3-c]Pyrazole Derivative with Potent and Selective Anticancer Effects In Vitro. Biology (Basel) [Internet]. MDPI; 2022 [cited 2022 Sep 24];11. Available from: /pmc/articles/PMC9219615/

97. Archna, Pathania S, Chawla PA. Thiophene-based derivatives as anticancer agents: An overview on decade's work. Bioorg Chem. Academic Press; 2020;101:104026.

98. Dhillon AS, Hagan S, Rath O, Kolch W. MAP kinase signalling pathways in cancer. Oncogene 2007 26:22 [Internet]. Nature Publishing Group; 2007 [cited 2022 Oct 4];26:3279–90. Available from: https://www.nature.com/articles/1210421

99. Lv C, Hong Y, Miao L, Li C, Xu G, Wei S, et al. Wentilactone A as a novel potential antitumor agent induces apoptosis and G2/M arrest of human lung carcinoma cells, and is mediated by HRas-GTP accumulation to excessively activate the Ras/Raf/ERK/p53-p21 pathway. Cell Death Dis [Internet]. Nature Publishing Group; 2013 [cited 2022 Oct 4];4:e952. Available from: /pmc/articles/PMC3877555/

100. Huynh J, Chand A, Gough D, Ernst M. Therapeutically exploiting STAT3 activity in cancer — using tissue repair as a road map. Nat Rev Cancer [Internet]. Available from: https://doi.org/10.1038/

101. Xiao X, Li BX, Mitton B, Ikeda A, Sakamoto KM. Curr Cancer Drug Targets. 2010.

102. Kamran MZ, Patil P, Gude RP. Advanced Centre for Treatment, Research & Education in Cancer (ACTREC). Biomed Res Int [Internet]. Hindawi Publishing Corporation; 2013;2013. Available from: http://dx.

APPENDIX

EXPERIMENTAL PIPERIDONES

Stock solutions of both 2608 (1-dichloroacetyl − 3,5-bis(3,4-difluorobenzylidene)-4-piperidone), 2610 (1-dichloroacetyl-3,5-bis(3,4-dichlorobenzylidene)-4-piperidone) and F8 (methyl 5-[(dimethylamino)carbonyl]-4-methyl-2-[(3-phenyl-2-propynoyl)amino]-3-thiophenecarboxylate) thiophene and piperidones were initially prepared in dimethyl sulfoxide (DMSO; Sigma-Aldrich, St Louis, MO, USA), and then, further working dilutions were also made using DMSO as a solvent. As necessary, aliquots of the piperidones were added directly to 24- or 96-well experimental plates containing cells cultured in a complete growth medium. DMSO, the piperidone diluent, was consistently tested at the same concentration as contained in the experimental samples as a control for non-specific solvent effects.

CELL CULTURE

Cell tissue cultures were obtained through the American Type Culture Collection (ATCC, Manassas, VA, USA). For the culture of lymphoma and leukemia, T lymphoblast CEM (ATCC ®CRL-2265™), B lymphocyte RAMOS (ATCC ®CRL-1596™), and promyelocytic leukemia HL-60 (ATCC ®CCL-240™), multiple myeloma MM.1R (ATCC ®CRL-2975™), MM.1 S (ATCC ®CRL-2974™), U266 (ATCC ®TIB-196™), and RPMI-8226 (ATCC ®CRM-CCL-155™), along with colon cancer (COLO 205, ATCC ®CCL-222™), the RPMI-1640 medium (Hyclone, Logan UT, USA), supplemented 10% fetal bovine serum (FBS, Hyclone), 100 U/mL of penicillin and 100 µg/mL of streptomycin (Thermo Fisher Scientific Inc. Rockford, IL) was utilized. The

HL-60 cells were grown using the above medium but with 20% FBS instead of 10%. The Hs-27 (ATCC ®CRL-1634™), MDA-MB-231 (ATCC ®CRM-HTB-26™), and PANC-1 (ATCC ®CRL-1469™) cell lines were grown in Dulbecco's Modified Eagle's Medium (DMEM; CORNING, Corning, NY, USA) with the addition of 10% FBS and 100 U/mL of penicillin and 100 µg/mL of streptomycin. A colorectal adenocarcinoma, HT-29 (ATCC ®HTB-38™), was cultured in McCoy's 5 A Medium supplemented with 10% FBS and 100 Units/mL Penicillin and 100 µg/mL Streptomycin. For colon fibroblast CCD-112-CoN (ATCC ®CRL-1541™), Eagles Minimum Essential Medium supplemented with 10% FBS, 100 Units/mL Penicillin and 100 µg/mL Streptomycin was used. Furthermore, MCF10A cells were grown in DMEM F12 supplemented with 10% FBS, 100 Units/mL Penicillin and 100 µg/mL Streptomycin. Lastly, pancreatic carcinoma (PC-3, ATCC ®CRL-1435™) utilized F-12 K Medium supplemented with 10% FBS, 100 Units/mL Penicillin and 100 µg/mL Streptomycin. Consistently, all cell types were incubated at 37ºC in a humidified atmosphere of 5% CO_2 using a conventional water-jacketed incubator.

STATISTICAL ANALYSES

Every experimental point indicates a minimum of three independent measurements unless otherwise stated. The findings were displayed as the average of the several measurements with their corresponding standard deviations to denote the experimental variability. The Linear Interpolator software was utilized to obtain the 50% cytotoxic concentration (CC_{50}) (https://www.johndcook.com/interpolator.html; accessed on 24 February 2022). Here, the CC_{50} is defined as the compound's concentration required to kill 50% of the cell population. The *P*-values were calculated using a two-tailed paired

Student's *t*-test to establish statistical significance between two samples, using the *T*-Test Calculator for 2 Independent Means software (https://www.socscistatistics.com/tests/studentttest/default2.aspx; accessed on 24 February 2022). On some circumstances, the significant *P*-values (≤ 0.05) were annotated with asterisks; * $P < 0.05$, ** $P < 0.01$, and *** $P < 0.001$.

CURRICULUM VITA

Risa Mia Swain received her Bachelor of Science in Microbiology from the University of Texas at El Paso (UTEP) in 2017. In Fall 2018, she joined the Biological Sciences PhD program at UTEP under the mentorship of Dr. Renato J. Aguilera. During her doctoral career, she attained one first author paper.

Ms. Swain attained funding through teaching assistant opportunities and gained experience with various laboratories. Displaying versatility and ability to adapt and learn in new environments.

Contact Information: utseabee89@gmail.com